AD_____

Award Number:

W81XWH-09-1-0443

TITLE:

Blockade of Nociceptin Signaling Reduces Biochemical, Structural and Cognitive Deficits after Traumatic Brain Injury

PRINCIPAL INVESTIGATOR:

Kelly M. Standifer, PhD, Hibah O. Awwad, PhD, Vanessa I Ramirez, MS, Courtney Donica, BS, Larry Gonzalez, PhD, Vibhudutta Awasthi, PhD, Paul Tompkins, PhD., Daniel Brackett, Megan Lerner.

CONTRACTING ORGANIZATION:

University of Oklahoma

Oklahoma City, OK 73104-5140

REPORT DATE:

July, 2010

TYPE OF REPORT:

Annual report

PREPARED FOR: **U.S. Army Medical Research and Materiel Command**
Fort Detrick, Maryland 21702-5012

DISTRIBUTION STATEMENT:

[X] Approved for public release; distribution unlimited

The views, opinions and/or findings contained in this report are those of the author(s) and should not be construed as an official Department of the Army position, policy or decision unless so designated by other documentation.

REPORT DOCUMENTATION PAGE

Form Approved
OMB No. 0704-0188

Public reporting burden for this collection of information is estimated to average 1 hour per response, including the time for reviewing instructions, searching existing data sources, gathering and maintaining the data needed, and completing and reviewing this collection of information. Send comments regarding this burden estimate or any other aspect of this collection of information, including suggestions for reducing this burden to Department of Defense, Washington Headquarters Services, Directorate for Information Operations and Reports (0704-0188), 1215 Jefferson Davis Highway, Suite 1204, Arlington, VA 22202-4302. Respondents should be aware that notwithstanding any other provision of law, no person shall be subject to any penalty for failing to comply with a collection of information if it does not display a currently valid OMB control number. **PLEASE DO NOT RETURN YOUR FORM TO THE ABOVE ADDRESS.**

1. REPORT DATE *(DD-MM-YYYY)*	2. REPORT TYPE	3. DATES COVERED *(From - To)*
01-07-2010	Annual	1 July 2009 - 30 June 2010

4. TITLE AND SUBTITLE

Blockade of Nociceptin Signaling Reduces Biochemical, Structural and Cognitive Deficits after Traumatic Brain Injury

5a. CONTRACT NUMBER

5b. GRANT NUMBER
W81XWH-09-1-0443

5c. PROGRAM ELEMENT NUMBER

6. AUTHOR(S)

Kelly Standifer, PhD, Hibah Awwad, PhD, Larry Gonzalez, PhD, Vibhudutta Awasthi, PhD, Vanessa Ramirez, MS, Courtney Donica, PhD, Paul Tompkins, PhD, Daniel Brackett and Megan Lerner.

5d. PROJECT NUMBER

5e. TASK NUMBER

5f. WORK UNIT NUMBER

7. PERFORMING ORGANIZATION NAME(S) AND ADDRESS(ES)

University of Oklahoma

Oklahoma City, OK 73104-5140

8. PERFORMING ORGANIZATION REPORT NUMBER

9. SPONSORING / MONITORING AGENCY NAME(S) AND ADDRESS(ES)

U.S. Army Medical Research and
And Materiel Command
Fort Detrick, Maryland 21702- 5012

10. SPONSOR/MONITOR'S ACRONYM(S)

11. SPONSOR/MONITOR'S REPORT NUMBER(S)

12. DISTRIBUTION / AVAILABILITY STATEMENT

I. Approved for public release; distribution unlimited

13. SUPPLEMENTARY NOTES

14. ABSTRACT

Protecting military personnel from blast-induced traumatic brain injury (TBI) has been a tremendous challenge. TBI results in hypoxia and ischemia reperfusion injury to the brain. Nociceptin (Noc), an endogenous peptide, is upregulated within one hour of TBI, impairs cerebral reactivity and exacerbates TBI by activating proapoptotic cascades. Long term neuroprotection involves inhibition of NFκappaB (NFkB). We hypothesized that activation of NFkB by the elevated Noc following blast-induced TBI contributes to metabolic and cellular changes underlying the appearance of neuronal and cognitive defects. Our objective was to determine if ORL1 antagonists will be neuroprotective against NFkB activation in a blast-induced TBI rat model and in cultured neuronal cells. TBI was simulated by shock tube to the head or chest; both reduced cerebral glucose uptake, especially to the thalamus, hippocampus and cerebellum as determined by 18-F-FDG uptake and PET imaging. Brain blast (80 psi) significantly reduced vestibulomotor function as determined with rotarod. Brain tissue histology revealed that markers for apoptosis and reactive gliosis were significantly elevated in the cerebellum and Noc levels trended towards significance. Apoptotic and neuronal injury markers were also elevated in sensory and motor cortex, consistent with the blast and the behavioral deficits measured. Cognitive defects were assessed using Morris water maze (MWM). NFkB activation by Noc was demonstrated by an NFkB reporter gene assay in SH-SY5Y and NG108-15 neuroblastoma cells. Noc also stimulated NFkB binding to DNA that was specifically blocked by ORL1 antagonism, and Noc also activated RSK signaling cascades in both cell lines.

15. SUBJECT TERMS Nociceptin, ORL1, Morris Water maze, traumatic brain injury, PET imaging, pressure blast, RISK cascade, NFkB

16. SECURITY CLASSIFICATION OF:			17. LIMITATION OF ABSTRACT	18. NUMBER OF PAGES	19a. NAME OF RESPONSIBLE PERSON
a. REPORT	b. ABSTRACT	c. THIS PAGE			19b. TELEPHONE NUMBER *(include area code)*
U	U	U	UU	53	USAMRMC

Standard Form 298 (Rev. 8-98)
Prescribed by ANSI Std. Z39.18

Table of Contents

INTRODUCTION:

Blast-induced traumatic brain injury (bTBI) is the most common injury of modern warfare. In 2008, nearly 25,000 U.S. soldiers were diagnosed with TBI, and the numbers are increasing with the ongoing warfare in Iraq and Afghanistan. However, numbers are estimated to be much higher, according to a recent publication that nearly 320,000 service members are exposed to TBI, with only 43% having been evaluated and documented by a physician (Rosenfeld and Ford, 2010). Neuronal and behavioral deficits are detected up to one year post-blast. Research is only beginning to reveal the mechanisms of bTBI. TBI reduces cerebral blood flow (CBF) and initiates a cascade of intracellular signaling events that result in neuronal damage and cognitive deficits (DeWitt et al, 2009). These signaling events require activation of NFκB, a transcription factor that regulates the expression of many genes. TBI induced by percussive or stab injuries also increases synthesis and release of the endogenous peptide nociceptin (Noc) that contributes to ischemia (Armstead 2000a, b; Armstead, 2002; Witt et al, 2003); antagonism of Noc actions relieves this impaired arterial dilation (Ross and Armstead, 2005). Further, impairment of cerebral vasodilation and the resulting hypoxia/ischemia also is inhibited by ERK and JNK inhibitors as well as by ORL1 antagonism (Ross and Armstead, 2005), strongly suggesting that elevated levels Noc resulting from TBI inhibit cerebrovasodilation and activate RISK signaling cascades associated with hypoxia and ischemia reperfusion injury. The novelty of our proposal is treating blast-induced moderate TBI early with a Noc receptor (known as ORL1) antagonist as a pharmacotherapeutic agent to prevent or reduce the biochemical, structural and cognitive deficits associated with mTBI by blocking initiation or propagation of Noc-mediated signaling cascades. ORL1 antagonists have limited side effects in rodents, suggesting that they could be rapidly administered in the field to prevent neuronal damage to the blast victim. To our knowledge, this is the first proposal to test the hypothesis that blockade of Noc-mediated signaling cascades following bTBI is neuroprotective, and that activation of NFκB by Noc in animals following bTBI contributes to metabolic and cellular changes underlying the appearance of cognitive deficits. Our research plan is designed to answer two primary questions: 1) Will treatment with an ORL1 antagonist will reduce biochemical, structural and cognitive deficits following blast exposure in male rats, and 2) Will Noc signaling through ORL1 activate those cascades implicated in ischemia following TBI (NFκB and reperfusion injury survival kinase (RISK) signaling cascades)? These studies have been and continue to be performed in rodent and human neuronal cell lines, and also will determine if ORL1 antagonists block downstream gene transcription subsequent to enzyme activation.

BODY:

Task 1a was to optimize blast conditions to ensure consistent production of mTBI based upon significant deficits in Morris Water Maze and/or novel object recognition performance in a blast group so that experiments with the full set of 4 groups can be initiated. **Task 1b** was to optimize conditions for immunocytochemical and immunoblotting experiments. **Tasks 8, 9, 10, 11 and 12** were to cryosection brains, perform immunocytochemical detection of markers for apoptosis (caspase-3; TUNEL), neuronal injury (amyloid precursor protein), NFκB activation (nuclear localization of subunit) and Noc expression. To collect and analyze immunocytochemical data, prepare images for manuscript, and prepare and submit manuscript, respectively.

A current essential task in the medical research field is to understand the mechanisms of blast-induced traumatic brain injury (bTBI). The complex nature of the blast components, both physical and chemical make it difficult to reproduce the exact blast conditions in the research laboratory using animal models. Ongoing efforts are currently trying to implement methods that will standardize animal blast models and conditions that will help us isolate the different components of the blast and better understand the mechanisms of bTBI. Research has documented various types of injury that could result from exposures to blasts ranging between primary (direct pressure effects), secondary (flying objects), tertiary (flying into objects) and quaternary (blast-related illnesses) injuries (DePalma et al., 2005; Ling et al., 2009; Leung et al., 2008). The various theories of the mechanisms for primary bTBI seem to fall into three categories: a pressure wave component that directly affects the brain transcranium, a physical mechanical insult to the brain that results in acceleration/rotation of the head solely due to the pressure waves affecting the brain via the CSF, and a thoracic mechanism whereby the blast pressure wave causes brain injury indirectly through the lungs via the vascular system (Cernak, et al.,

2005; Courtney and Courtney, 2009; Saljo et al., 2010; Hicks et al., 2010; Risling et al., 2010). Our blast model utilizes a pressure wave generator that simulates the primary blast injury due to the pressure wave component, without any further external insult or any mechanical rotational/torsion effect. The blast pressure wave generator was developed and utilized for blast studies by our collaborators (Irwin et al, 1997). Eliminating effects of external injury and mechanical impact from the effect of blast pressure alone allows us to further our understanding of blast-induced traumatic brain injury.

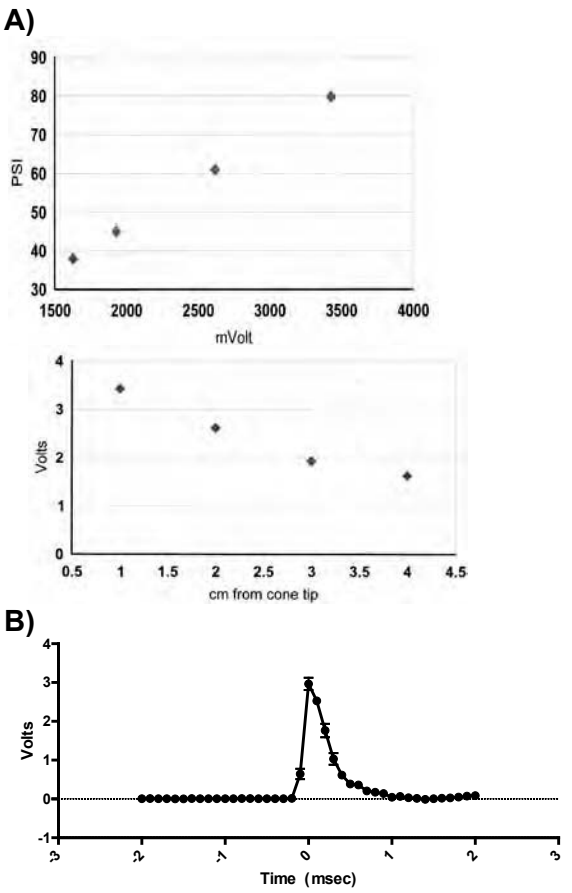

Fig 1. Blast wave overpressure. Calibration curves were performed per manufacturer's instructions for converting Volt values recorded by the transducer into psi pressure values (A: upper panel); Pressure values were varied by changing the distance of the transducer from the blast nozzle in increments of 1 cm (lower panel). B) An overpressure peak representative of four different blasts. Indicated values were recorded from the transducer every 0.1 msec. Post-blast negative pressure values were very minimal and reached -0.03V and appeared around 1.3-1.6 msec following the peak pressure. (N=4)

The blast generator was calibrated and tested to optimize the reproducibility of our blast conditions by recording pressure wave measurements every 0.1 ms using a piezoelectric transducer (Piezotronics, Inc.). Calibration curves were performed according to the manufacturer's recommendations as shown in Fig. 1A. Figure 1B shows the pressure wave curve generated with the blast generator nozzle positioned 2 cm from the transducer for four consecutive trials. Based on our calibration curves and measurements, rats subjected to a single blast at a distance of 2 cm from the nozzle were exposed to pressures of approximately 60 psi over 2-3 ms. A recent study by Svetlov et al (2010) addressed the issue of having a model of controlled blast over pressure animal models. They recommended placing the animal under the blast nozzle and not horizontally along the axis of the nozzle to prevent the impact of the venting gas from the blast generator. Also, they recommended calibrating the blast wave measurements by a transducer alone without the rat being under it. These results confirm that our blast generator produces reproducible blast pressure waves with little variability between blasts.

The first aim of this project was to measure cognitive function using the Morris Water Maze (MWM). The MWM is a cognitive test that measures spatial memory using a circular pool with a hidden platform located below water level. Rats learn the position of the platform based on visual distal cues in the room. Delay in learning the location of the submerged platform or in remembering where it was is indicative of a cognitive impairment in learning and/or memory. With reports of blast-induced deficits in motor function (Long et al., 2009) and visual impairment (Petras et al., 1997) it was necessary to confirm that the blast conditions did not affect the ability of our rats to swim or see, even though it is commonly accepted that rat motor function on land does not necessarily correlate with swimming ability. This was important to address because any blast-induced effect on motor function would make it difficult to interpret whether the differences in MWM performance are the result of deficits in motor function or cognitive function. Therefore, the first experiment was performed to answer this question. Rat studies were initiated after OUHSC IACUC and ACURO approvals were received, 8/6/2009. The cued navigation MWM with a visible raised white platform (1cm above water level) with a white flag was used to assess both swimming ability and vision. The rotarod was chosen as a metric for motor function since non-blast TBI studies indicate that the rotarod is the most sensitive vestibulomotor test, such that it detects deficits even when beam balance and beam walk assays indicate that the animal has recovered (Hamm et al., 2001). Furthermore, recent studies on the comorbidity of vestibular pathology and TBI in veterans confirmed the importance of

understanding vestibulomotor effects of blast-induced TBI (Scherer and Schubert, 2009; Bottshall and Hoffer, 2010; Fausti et al., 2009).

Methods:

Sprague-Dawley male rats (225-250g) were purchased from Charles River Laboratories International Inc., MA. Animals were housed in pairs with ad libitum access to food and water, with 12h dark/light cycle. All protocols used were approved by OUHSC's Animal Use and Care Committee.

Rotarod performance: On day 1, rats were habituated with the apparatus for 30 s, then trained at 3 rpm for 10 min. On day 2, rats were given 1 trial at 3 rpm, followed by 3 trials at 10 rpm and one final trial at 20 rpm. All consecutive trials had 5 min inter-trial intervals. If the rat reached criterion (180 s on rotarod continuously without falling), it was moved on to the next speed. Days 3 and 4 were test days, where the rats were given 3 trials with 15 min inter-trial intervals. Rotarod speed was continuously increased during each test trial as follows: 5 s at 3 rpm, then speed was manually increased to 10 rpm over 5 s, after 15 s, the speed was increased in increments of 5 rpm over 5 s and maintained for another 15 s, until speed reached 30 rpm, at which speed was maintained until rat fell off the rotarod or reached criterion. The average time each rat spent on the rotarod for all 3 trials on the final test day was taken as their pre-blast value. Rats performing less than 45 s were excluded from the study. The same 3 test trials were done on days 1-4, 7 and 8 post-blast.

Blast-Induced Traumatic Brain Injury (bTBI) method: Rats were group-matched based on rotarod performance and weight. Rats were anesthetized with isoflurane (induction with 4 min of 4% isoflurane/70% N_2O; maintenance with 2.5% isoflurane) and secured in the supine position to a foam pad with elastic properties to prevent the concussive effects from the hard surface below. The foam is contoured to the animal's shape so that it rests in the foam. The animal is positioned such that the blast wave generator nozzle is centered directly over the head. Sham rats received anesthesia without blast, whereas the other 2 groups were exposed to either a single 60 or 80 psi blast from the blast-pressure wave generator described (Irwin et al., 1998: see appendix). In some animals (as indicated per the experiment below) the chest was shielded from the blast by a 2 mm thick piece of metal plating to prevent damage to air filled organs such as lung, liver and kidney; other animals received a single 45 psi blast to the chest, unprotected. The anesthesia nose mask was removed just prior to initiation of the blast. Personnel wore ear muffs (NRF 20) during the administration of the blast pressure wave as a protection against the noise of the blast (maximum 100 dB). The time it took for rats to awaken after blast and/or anesthesia alone was recorded for every rat as recovery time.

Cued Navigation Morris Water Maze (MWM) method: Rats were tested in a large circular water maze (6 ft diameter), with water level of 30 cm at 25 ± 1ºC. The top half of the water tank was painted black, and the water was mixed with nontoxic Tempera black paint. The visible platform (island) extended 1 cm above the surface of the water, with a flag attached 7 cm above the platform using a copper wire. Visual cues were absent. Each rat received 4 trials to reach the visible platform in the MWM from 4 different entry points. Trials ended after 120 s or upon finding the platform. Cued navigation was monitored and recorded as latency to reach the island using the video-tracking software ANY-maze (Stoelting Inc.). Each animal was allowed to remain on the island for 30 sec after reaching the island then tested for the next trial after a 30 s interval.

Matching-to-sample spatial working memory Morris Water Maze (MWM) method: Rats were tested in the same water maze described above. However, the circular platform (island, 10 cm diameter) was hidden 2 cm below the surface of the water and visual cues were present. Each rat received 2 identical trials to find the hidden platform in the MWM using the schedule in the attached Nature Protocol by Vorhees et al. (2006; see appendix), such that the second trial is the matching-to-sample working memory. Trials ended after 120 s or upon finding the platform. If rats did not locate the platform, they were manually guided to the platform. Rat navigation was monitored and recorded as latency to reach the island using the video-tracking software ANY-maze (Stoelting Inc.). Other measures also were determined by the software as indicated in the appropriate figure legends.

Immunohistochemical staining: On days 2 and 9 post-blast, brains were extracted and fixed in 10% neutral buffered formalin. Brains were sliced into 3 mm coronal sections that were further processed and paraffin embedded. Slices (5 µm) from sham and 80 psi blast groups (2 rats each) representing the cortex and cerebellum at Bregma -3.8 and -11.3mm respectively (Paxinos & Watson stereotaxic coordinates) were deparaffinized and rehydrated. Slides were immunostained for reactive astrocytes and apoptotic cells using glial fibrillary acidic protein (GFAP; Thermoscientific Inc.; ready to use dilution) and cleaved caspase 3 (Cell Signaling; 1:200 dilution) antibodies respectively. Anti-nociceptin antibody (sc-9763; Santa Cruz; 1:200 dilution) and APP antibody (ab15272; Abcam; 1:100 dilution) were used to detect Noc and the neuronal axonal injury marker amyloid precursor protein (APP), respectively. Peroxidase visualization was developed by NovaRED™ (Vector Laboratories) and counterstained with ImmunoMaster Hematoxylin (AmericanMaster Tech Scientific, Inc., Lodi, CA, USA). Slides were then mounted with coverslips using Acrymount. Images were captured with light-transmitted brightfield setting using an Axioplan 2 Zeiss microscope equipped with a motorized Bacus Laboratories Inc. Slide Scanner (BLISS). Quantification of images captured at 200x magnification was performed on 15-23 images/region/rat as described (Lehr et al., 1999). GFAP images in the cerebellum were coded and counted by two individuals in a blind manner.

Statistical Analysis: Data were analyzed using the appropriate statistical test as indicated in the figure legends. Both Graphpad prism software v5.0 and SAS v9.1 were used as the statistics software

Results

Rats subjected to either 60 or 80 psi blasts did not show a significant difference in recovery time from blast compared to sham rats (Fig 2). This indicates that our blast conditions do not cause any further short-term effects on the parasympathetic vagal system compared to sham rats that received anesthesia without blast. Rotarod performance between the three groups indicated that there was a pressure-dependent bTBI vestibulomotor effect compared to pre-blast rotarod performance. The 80 psi blast group showed a significant reduction in rotarod performance denoted by reduced time spent on the rotarod (Fig. 3, *P<0.05). This difference was not seen with the 60 psi blast group. Our findings therefore suggest a threshold pressure value between 60 and 80 psi at which defects in vestibulomotor function can be detected. These findings could potentially become a clinical landmark for healthcare professionals in the field. For example, if human threshold values could be extrapolated from animal studies, then pressure sensors worn by war fighters would detect exposure to threshold values, thus ensuring they were screened for vestibular effects and treated accordingly.

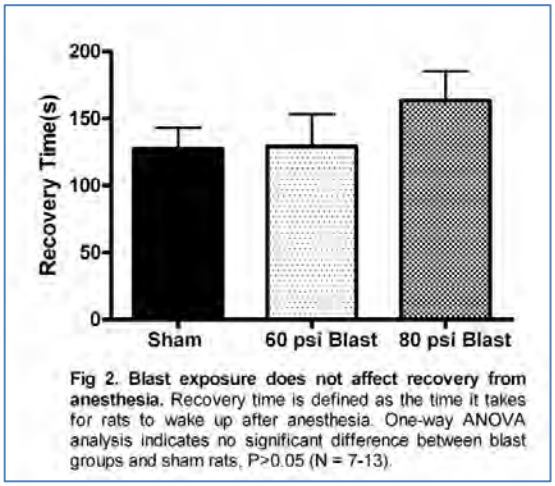

Fig 2. Blast exposure does not affect recovery from anesthesia. Recovery time is defined as the time it takes for rats to wake up after anesthesia. One-way ANOVA analysis indicates no significant difference between blast groups and sham rats, P>0.05 (N = 7-13).

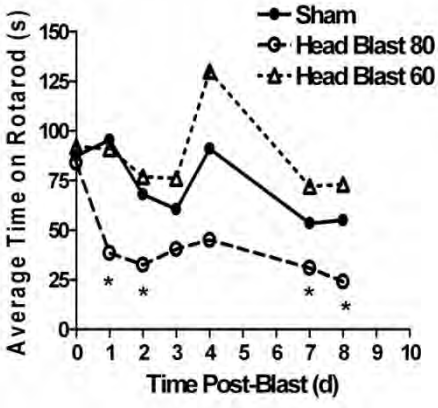

Fig. 3. Rotarod performance was reduced by 80, but not 60, psi blast pressure to the head All rats were pretarined on the rotarod for 3 days as indicated in Methods. Rotarod performance was measured on days 1-4, 7 and 8 post-blast and the average of 3 trials were calculated/day. Data are represented as median value/group. The 80 psi blast times were significantly different from pre-blast values (day 0) per Friedman 2-way non-parametric ANOVA (*p<0.05). Repeated measures ANOVA with Bonferroni post-hoc test indicates that the 80 psi group significantly differs from both sham and 60 psi groups across days, p<0.05; 60 psi blast group does not differ from the sham group.

These findings were very interesting, but we also were looking for a cognitive deficit to be determined by performance in the MWM post-blast. Therefore, a direct swimming test was done using the cued navigation MWM (Fig. 4) as explained in the methods section. The latency time for the rats to reach the visible island did not differ between the 3 groups. This indicates that the blast treatment did not alter the ability of the animals to see the platform and swim to it as early as one day post-blast, despite the fact that their vestibulomotor function on the rotarod was reduced. Since general vision and swimming motor function is unaltered by 60 or 80 psi blasts, we felt that we could perform the MWM tests without fear of those factors influencing our results. This test was performed for

each animal in all our experiments to ensure their swimming and visual abilities as an inclusion criterion. To date, none of our blast animals have been excluded based on this metric.

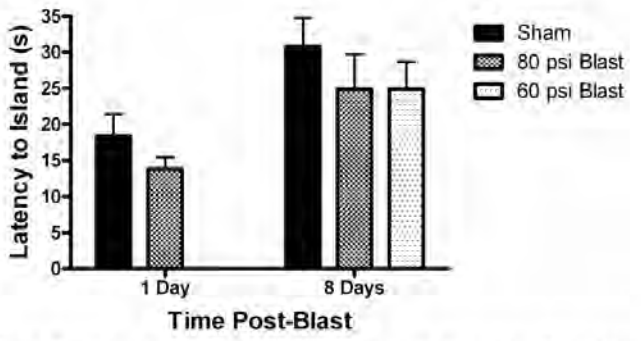

Fig 4. Cued navigation Morris Water Maze activity is not affected by blast exposure. Swimming motor function was measured by timing latency of the rat to reach a visible platform. There were no differences between the three groups in latency time at Day 1 (N=12; unpaired Student's t-test, P>0.05) or Day 8 (N=7-8, One-way ANOVA, P>0.05).

The interesting pressure-dependent effect of our blast on the vestibulomotor function led us to examine the two brain regions associated with vestibulomotor function, the cortex and the cerebellum. On day 9 post-blast, rats were euthanized and their brains removed, fixed and paraffin-embedded for immunohistochemistry as detailed in the methods section. Immunoreactivity of the reactive astrocyte marker, GFAP, the neuron axonal injury marker, amyloid precursor protein (APP), the neuropeptide Noc, and the activated trigger for apoptosis, cleaved caspase 3, were quantified in the cerebral cortex (motor and sensory areas) and in the cerebellum. Images representative of the median quantified value for each marker are shown for both the sham and the 80 psi blast group (which shows the vestibulomotor function deficit) in Figs 5 and 6, with quantified results shown in Fig 7. Our findings indicate that GFAP and cleaved caspase 3 are increased in the cerebellum on day 9 post-blast, with no significant change in GFAP levels in the cerebral cortex compared to sham controls euthanized on the same day. APP immunoreactivity also was significantly increased in blast TBI

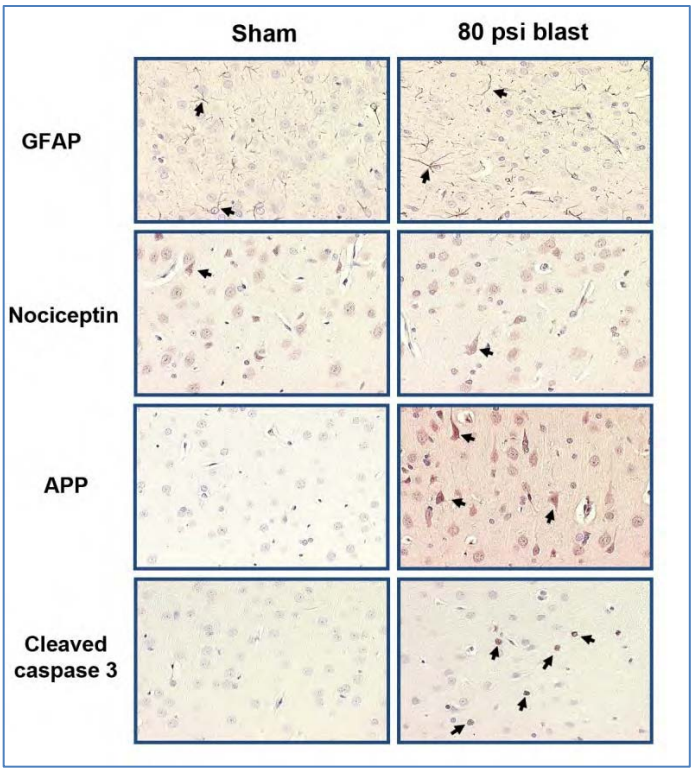

Fig 5: 80 psi blast does not alter GFAP expression in motor and sensory areas of the cerebral cortex, however it increases APP and cleaved caspase 3 expression in pyramidal cells. *GFAP, Noc, APP and cleaved caspase 3 immunoreactivity in coronal sections (5 µm) located at ~Bregma –3.8 mm (Paxinos & Watson). Representative images of sham and 80 psi bTBI rats are enlarged 200x. Black arrows indicate immunopositive cells in cortex. Quantification is provided in Fig. 7.*

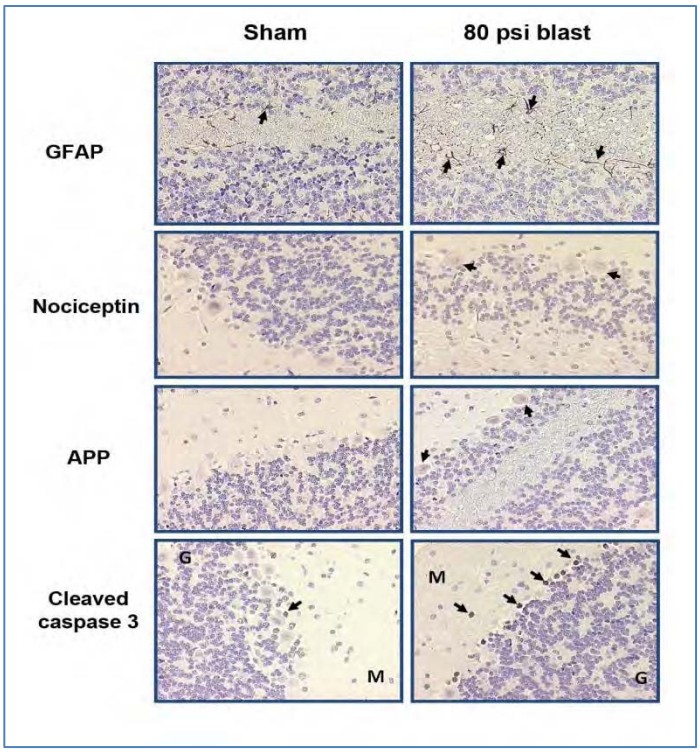

Fig 6. GFAP and Cleaved Caspase 3 Expression in cerebellum is increased by bTBI*. GFAP immunoreactivity (IR) in coronal sections (5 µm) from paraffin-embedded brain slices located at ~Bregma –11.3 mm. Representative images of GFAP, Noc, APP and caspase 3 IR from the cerebellum of sham and bTBI rats are enlarged 200x. Black arrows indicate positively labeled GFAP astrocytes or cleaved caspase 3 cells in the cerebellum. M: Molecular layer, G: Granular layer of the lobule. See Fig. 7 for quantification.*

rats compared to sham rats on day 9 post-blast in the cortex. No significant change in GFAP and cleaved caspase 3 immunoreactivity was detected in the cerebellum of day 2 post-blast animals (data not shown).

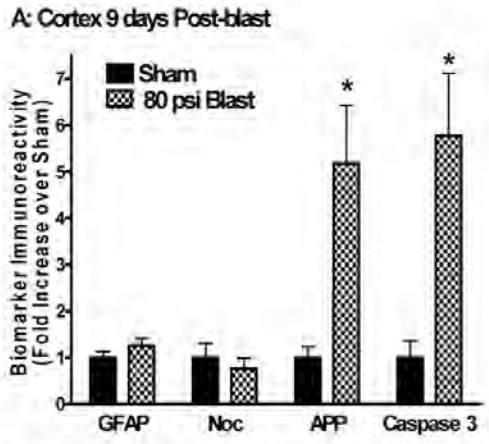

Fig 7. Quantification of changes in immunoreactivity. Protein expression was quantified from 15-18 images/region/rat using Photoshop as described in Methods, and is expressed as fold increase over sham rats from cerebellum and motor and sensory areas of the cerebral cortex. The ratio of positively-labeled pixels to total pixels per image were averaged per group of rats and normalized to ratios derived from sham rats (N=30-43 images). *Represents significant difference in immunoreactivity of bTBI group from sham group by unpaired Student's t-test, $P<0.05$.

Further analysis of other brain regions (e.g. hippocampus, thalamus, striatum) are currently being processed for expression of clinically relevant biomarkers (Svetlov et al., 2009; Leung et al., 2008), including S100B astrocytic marker, HNE (4-hydroxy-nonenal) oxidative stress marker, and activated NFkB (phosphor NFkB). Furthermore, the proteins that have shown signficicant changes post-blast will be co-labeled using immunofluorescence with GFAP (reactive astrocyte) and Neu-N (neuronal) markers to determine the type of cells expressing these markers as well as cell type and location of blast-induced Noc expression.

Conclusions from Tasks 1a, 1b and 8-12:

Rotarod performance on days 1, 2, 7 and 8 post-blast in 80 psi blast-injured rats was significantly reduced compared to sham rats, whereas 60 psi blast did not reduce rotarod performance. This indicates that there are pressure-dependent effects resulting in depression of motor function, balance and coordination following bTBI. Cerebellar immunoreactivity of GFAP, a marker for reactive astrocytes and indicative of a response to damage or inflammation, was significantly increased in rats that received an 80 psi blast compared to sham rats. Noc immunoreactivity trended toward an increase in the cerebellum. Cleaved caspase-3 increase in the cerebellum of blast TBI rats 9 days post-blast suggests that 80 psi blast and/or Noc-induced reactive astrogliosis triggers pro-apoptotic pathways which further damage the central nervous system.

Our results indicate a direct link between blast-induced brain injury and an increase in reactive astrocytes in the cerebellum. This is the first study, to our knowledge, to show a pressure-dependent effect on rotarod performance as a measure of vestibulomotor function in bTBI. This is also finding from a memory perspective, where the cerebellum is now identified with a role in learning and memory as well as vestibulomotor functions (Mandolesi et al., 2001).

Blast-induced changes in cortical biomarkers manifested differently. Unlike in the cerebellum, GFAP immunoreactivity was unchanged in the sensory and motor cortices, however both APP and caspase 3 expression was significantly increased after 9 days post-blast. This suggests that while there are apoptotic cells in the motor cortex, they do not correlate with astrogliosis or enhanced Noc expression. Our immuno-histochemical results are very interesting data and support a recent study that also fails to see a significant change in the GFAP levels in the cortex following bTBI (Svetlov et al., 2010). To better quantify expression of these markers throughout each brain region, tissue from various brain regions will be dissected and prepared for immunoblotting as described in methods. Those experiments will confirm the changes seen with immunohistochemistry results.

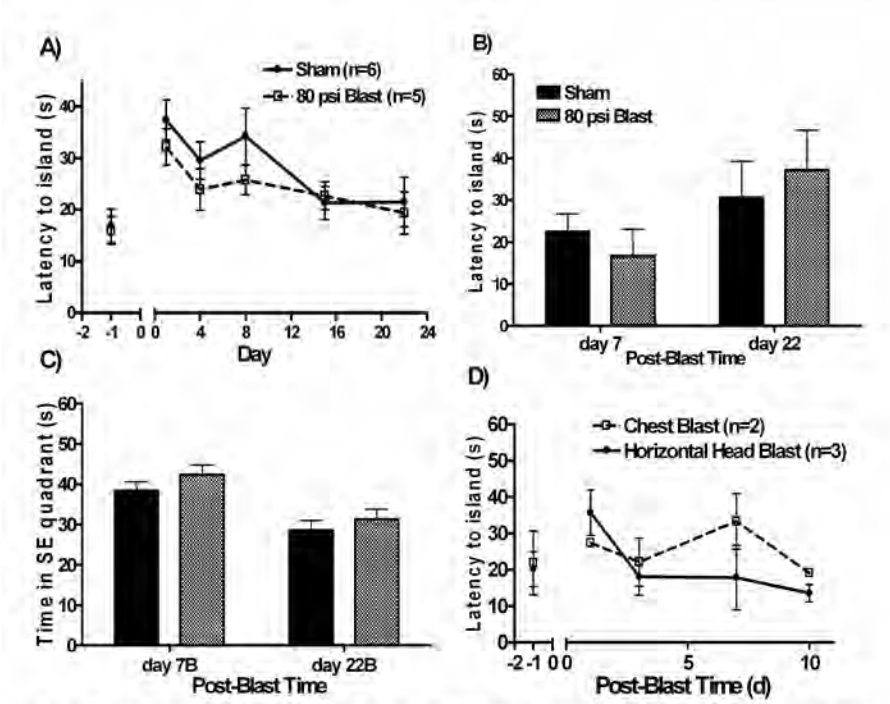

Fig. 8. Memory retention and relearning test. 80 psi bTBI rats did not show significant differences from the sham rats. Rats were trained pre-blast for 7 days to find the platform in a fixed location. Rats were then group-matched based on weight and performance and received either an 80 psi blast or sham blast + anesthesia the followind day. Day -1 represents performance on the last day of training. Ability to find the platform was monitored using ANY-maze software on days 1, 4, 8, 15 and 22 post-blast. Probe tests were performed both pre-blast and post-blast and B) both latency to island and C) time spent in SE quandrant (platform position during the training period) are represented. Data is presented as the average of all 4 trials for all rats in that group on that day.Two-way ANOVA statistical analysis ($P<0.05$). N=5-6. D) Sham rats from previous figures were used to test the effect of two blast conditions on relearning.

Next, after showing that our blast conditions did not produce measurable defects in vision or swimming motor function as demonstrated by the cued navigation MWM (Fig 4), spatial memory MWM experiments were performed. We initially studied the effect of the blast on memory retention using our collaborator's protocol (Dr. L. Gonzalez). All rats were trained for 7 days to locate the hidden platform (SE quadrant) until the performance of each rat reached an asymptote. A probe test was performed on day 7. Rats were excluded if they did not reach the criterion of locating the platform in less than 15s on 2 consecutive trials or if they did not spend >25% of the 90 sec probe time in the SE quadrant. Seven of the rats failed to meet criterion, so the remaining 11/18 rats were then group-matched based on weight into either sham or 80 psi blast group. Rats received the blast or sham blast the day after training was completed and then the platform location was changed and the rats received 4 trials/day on days 1, 4, 8, 15 and 22 post-blast. Latency to find the platform was recorded using ANY-Maze software and the average of all 4 trials is presented in Fig. 8.

We did not find any difference between the sham and the 80 psi blast to the head group when the 4 daily trials were averaged and analyzed over the full 22-day time course. These results were not what we expected to see, nor was it the short term effect of what has been reported in the literature (Saljo et al., 2009; Long et al., 2009). Therefore, we wanted to determine whether our blast conditions were too mild to see a cognitive deficit or whether the paradigm we used in Dr. Gonzalez's protocol needed to be changed.

To address the first question regarding our blast conditions, we chose the blast model publishes by our collaborators which documented cardiovascular effects of unprotected chest blasts (Irwin et al., 1997) and compared it to the 80 psi blast to the head where we had already documentd the vestibulomotor deficits (Fig. 3). A recent study compared the various blast exposure thresholds involved in traumatic brain injury mechanisms regarding the thoracic region and acceleration injury from a blast (Courtney and Courtney, 2010). This encouraged us to pursue the chest blast model, so we took the 6 sham rats from the previous experiment and exposed them to an 80 psi blast to the head with their body along the axis of the blast nozzle, or to a vertical 45 psi blast to the chest. These sham rats served as their own internal pre-blast controls since they already went through the previous training (Fig. 8D).

Effects of these two blast conditions on learning and memory can be tested by a variety of paradigms using the MWM (Cernak et al., 1999; Vorhees and Williams, 2006). Recent papers have highlighted the primary clinical cognitive differences between TBI and post-traumatic stress disorder (PTSD), indicating that war fighters suffering from TBI often suffer from explicit attention deficit in working memory among other TBI-related symptoms (Vasterling et al., 2009; Jaffee et al., 2009; Belanger et al., 2009; Huckans et al., 2010). Therefore, we chose to test the effect of head and chest bTBI as discussed above on the working memory protocol known as the matching-to-sample paradigm (Vorhees and Williams et al., 2006, Appendix). The sample trial (trial 1) consists of moving the location of the platform every day to a new loation, whereas the matching trial (trial 2) is identical to trial 1. These experiments were to determine the blast conditions showing the most consistent effects on cognitive function in order to pursue the ORL1 antagonist studies.

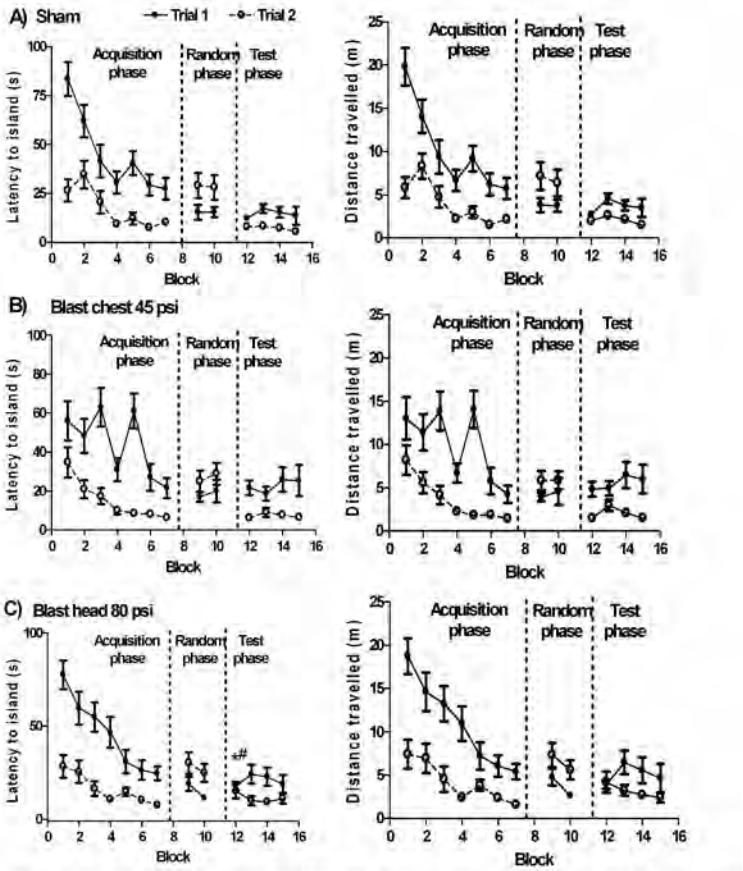

Figure 9. Working Memory MWM. Data from matching-to-sample MWM for each treatment group is presented on a separate panel. Trial 1 is the training trial and Trial 2 is the memory trial. Rats were exposed to sham blast (A), Chest blast (B) or Head blast (C) on day 0. They were then trained for the acquisition phase, followed by a random phase and a test phase. Latency to reach the island and distance travelled were measured and values for all rats in each group/trial is averaged into blocks of three day intervals. Statistical analysis was performed using 2-way ANOVA with Bonferroni post-hoc test (*P<0.05). Results were significantly different from same block of same trial in sham (A)* or significantly different from other blast group (B or C)#.

Trial 1 is a measure of the rats learning the task of finding a new location of the platform. Although all groups showed a gradual increase in learning the sample task over the 21 day period (7 blocks), there was a slight difference in the chest blast group's performance as illustrated in Fig. 9A-C. The chest blast group found the platform faster initially compared to the sham and head blast groups. However, their performance was very inconsistent over the training period. A two-way ANOVA with repeated measures analysis for each block shows that Block 5 (days 13-15 post-blast) is significantly different between the 2 blast groups, but not when compared to the sham group. Results from a general one-way ANOVA repeated measures analysis across blocks of each phase are represented in Table 1.

Trial 2 is a measure of the working memory. If rats remembered the previous trial based on the spatial cues, they should only use their working memory to repeat it. Therefore, rats should find the platform more quickly on trial 2 than on trial 1. The difference between the 2 trials is essentially the working memory, such that the bigger the difference the better the working memory. Over time, as the rats get better at the task in trial 1 the difference between trial 1 and 2 is reduced. Average speed across trials does not vary between groups (data not shown). Two way ANOVA test analysis reveals a significant difference in the difference between trials 1 and 2 between treatment groups.

Since we did not see a dramatic effect on working memory, the acquisition learning paradigm of the MWM protocol (Voorhees and Williams, 2006) was tested with the next group of rats. Rats were acclimated for 1 week and group-matched based on their weights. Eighteen rats were split into 3 groups (6/group): 80 psi blast to head, 45 psi blast to chest, and sham blast groups. One rat was excluded from the sham group at the end of the study due to hydrocephaly that was identified after brain extractions took place. Another rat died from the chest blast. In the learning paradigm, rats were trained to find the hidden platform located in the SW quadrant of the pool from 4 different entry points over 4 trials for 6 consecutive days (when they reach a performance

Table 1. One way repeated measures ANOVA analysis using post-hoc Neuman-Keuls Multiple Comparison Test

Latency to island (s) parameter						
	Acquisition phase (Blocks 1-7)		Random phase (Blocks 9-10)		Test phase (Blocks 12-15)	
	Trial 1	Trial 2	Trial 1	Trial 2	Trial 1	Trial 2
Sham v Chest Blast	NS	NS	NS	NS	*	NS
Sham v Head Blast	NS	NS	NS	NS	*	*
Head Blast v Chest Blast	NS	NS	NS	NS	NS	*
Distance travelled (m) parameter						
	Acquisition phase (Blocks 1-7)		Random phase (Blocks 9-10)		Test phase (Blocks 12-15)	
	Trial 1	Trial 2	Trial 1	Trial 2	Trial 1	Trial 2
Sham v Chest Blast	NS	NS	NS	NS	*	NS
Sham v Head Blast	NS	NS	NS	NS	*	NS
Head Blast v Chest Blast	NS	NS	NS	NS	NS	NS

asymptote). A probe test was done for 60 sec on day 7 after the platform was removed. All rats were able to learn the location of the platform within the 6-day training period, however there was a small but significant difference that could be detected between the chest blast group and the sham group on day 6 of training. This could be interpreted as a slight delayed cognitive deficit in the chest blast rats, however, these rats performed in a similar fashion in the probe test measure of "latency to island" (data not shown) indicating that they learned the location of the platform. Furthermore, the head blast group showed a slight trend of an increase in the probe test when measured by latency to island (data not shown), however with this group size (n=5-6), it hasn't reached significant difference. Therefore, it is too early to decide on the outcome of these results, since these experiments are usually done in a group size of at least 10-12 rats.

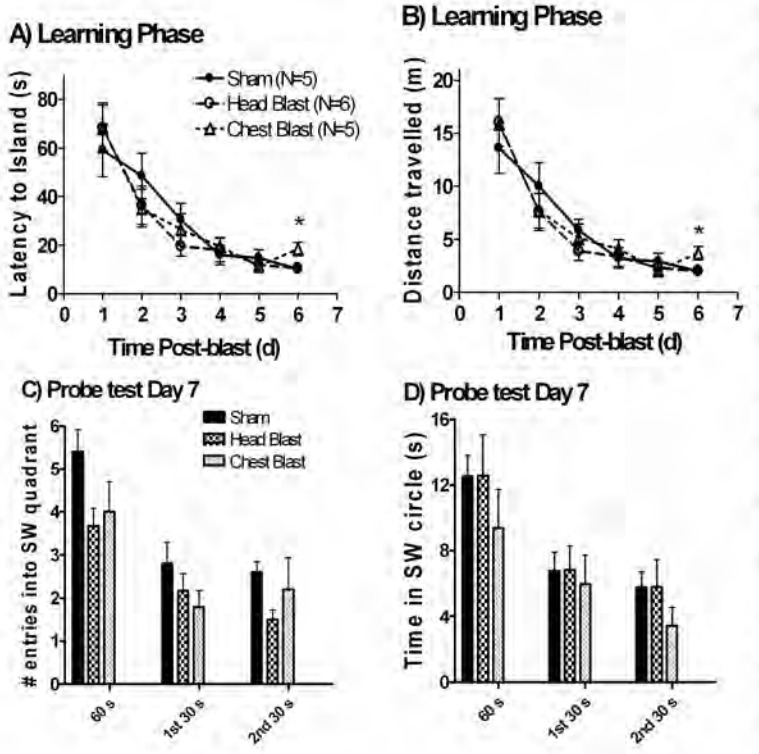

Fig. 10. Acquisition Learning learning was decreased with Chest Blast. Rats were group-matched based on weight and received either an 80 psi blast to the head, 45 psi blast to the chest, or sham blast on day 0. Rats were trained to find the platform in a fixed location (SW quadrant) over four trials/day for 6 days (24 trials total).Rats receiving a chest blast differed from sham and head blast on the last day of training (*p<0.05; Two-way ANOVA statistical analysis (P<0.05; N=5-6). Head blast rats show a slight increase in latency to island on the probe test trial 25, however a greater sample size is need to show significance. The platform was removed on day 7 and a 60-sec probe test was performed. Both blast groups had fewer entries into the SW quadrant, but it did not achieve significance with this sample size. ANY-maze software was used to calculate A) latency to island, B) distance travelled, C) # entries into the SW gradrant and D) time spent in the circular vicinity around the island. Data represents the average of all 4 trials for each rat in each group (A, B) or the average of all probe tests within each group (C, D).

Another set of experiments will be performed next month to increase sample size in order to determine a final outcome based on statistical significance. The blast group showing the cognitive deficit in this learning paradigm will then be used to continue our proposed experimental design to study the effect of ORL1 antagonist treatments on the blast-induced cognitive deficit.

Task 2 (a and b) and Task 3

Task 2a – Optimized treatment and testing times will be utilized for the full treatment protocol with 4 groups of rats (sham, blast, Noc antagonist and blast + antagonist). Four rats /group will be treated and tested each round, with half of the animals removed after behavioral testing on day 1 following the blast for PET imaging (FMISO and FDG). The remaining rats will be subjected to PET imaging after 5 -10 days, depending on the outcome of task 1. This will be repeated until n=4 for each PET isotope/group/testing day. Task 2b – After each imaging session, rats will be euthanized and brains will be removed and flash frozen until radiation levels reach background levels (4-6 days)

Changes in glucose metabolism are associated with many of the defects seen in traumatic brain injury in general (Gross eta l., 1996). More importantly, a recent study using FDG-PET imagine showed reduced cerebrocerebellar glucose metabolism in 12 Iraq war veterans (Peskind et al., 2010). Therefore, we next studied the changes in glucose uptake of the blast TBI rats by using quantitative positron emission tomography (PET) imaging compared to sham rats. Our first experiment utilized ^{18}F-fluorodeoxyglucose (^{18}F-FDG), which is an analog of glucose that the brain utilizes in a similar fashion to glucose. Therefore, glucose metabolism could be quantified by the uptake of ^{18}F-FDG in the brain. Our first study involved 12 rats divided into 3 groups, with 4 rats per group (sham, 80 psi blast to the head, and 45 psi blast to the chest). However, one rat died during imaging and was excluded, reducing the chest group size to 3.

Methods:

PET/CT imaging

Clinical grade ^{18}F-FDG was obtained by from IBA Molecular (Dallas, TX). PET imaging was performed in the Small Animal Imaging Facility (University of Oklahoma Health Sciences Center, College of Pharmacy) in rats deprived overnight of food, but not water. Rats were anesthetized with 2.5% isoflurane in the air stream during the imaging sessions. About 100 µCi (approximately 0.5 ml) of radiotracer was intravenously injected in the tail vein of each rat. After allowing the radiotracer to distribute for 45 min, the animals were again anesthetized and imaged for 45 min using X-PET machine (Gamma Medica-Ideas, Northridge, California, USA). After imaging, rats were euthanized and brains were excised. Brain-associated radioactivity was measured in a well γ-counter. The brains were then flash frozen in liquid nitrogen and transferred to a lead container in -80°C freezer for at least 1-2 days. The acquired image data were reconstructed using filtered back projection algorithm. A computed tomograph (CT) was also acquired to establish anatomic landmarks. Both PET and CT were fused together using Amira 3.1 software, Visage Imaging Inc. (San Diego, California, USA) provided with the imaging system. The accumulation of ^{18}F-

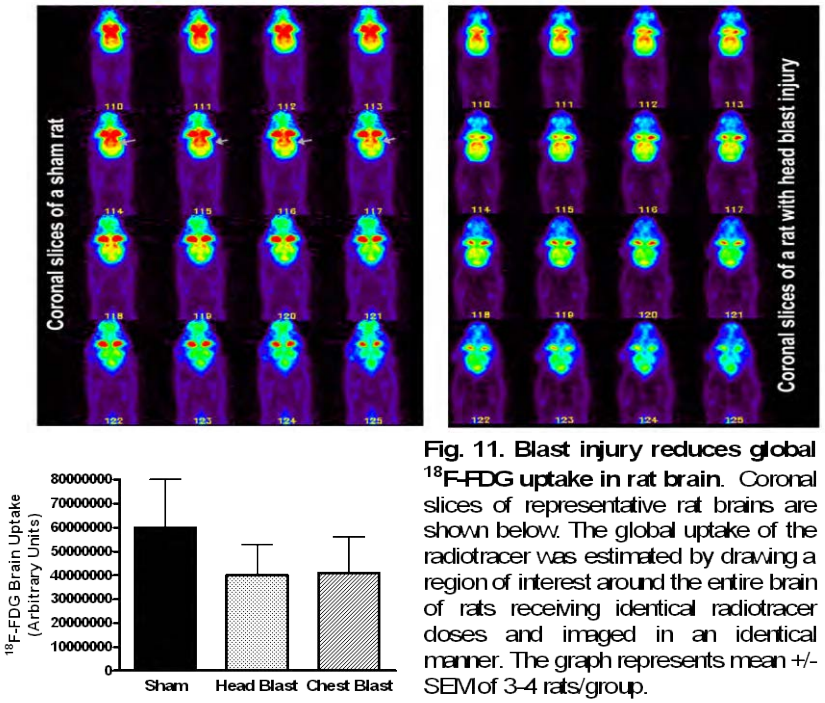

Fig. 11. Blast injury reduces global ^{18}F-FDG uptake in rat brain. Coronal slices of representative rat brains are shown below. The global uptake of the radiotracer was estimated by drawing a region of interest around the entire brain of rats receiving identical radiotracer doses and imaged in an identical manner. The graph represents mean +/- SEM of 3-4 rats/group.

FDG was estimated by drawing regions of interest around the volume images corresponding to the entire brain region as described (Awasthi et al. 2010 J Nucl Med). To eliminate the effects of various blast conditions on glucose metabolism in non-CNS regions (e.g. liver, kidney, muscle), CNS uptake was not normalized to total serum ^{18}F-FDG. The same amount of radiotracer was injected into each animal, all animals were same size and weight and our primary question was to determine differences in amount of ^{18}F-FDG within the brain and determine the location of those differences.

Plasma Glucose Collection and Assay:

Blood samples of 100 µl were collected in a heparinized tube from the tail vein immediately prior to and from the heart immediately after PET imaging while still anesthetized and spun at 2000rpm for 5 min. Pre-imaging and post-imaging plasma samples of 25 µl (supernatant) were collected and stored at -20°C for glucose counts and another 25 µl of both plasma samples were also collected in another tube for counting radioactivity levels. Plasma samples were counted in the well γ-counter for a total of 5 min. At the end of each day, plasma samples from all 4 rats were thawed and assayed for glucose content using Quantichrom assay kit (BioAssay Systems, DiGL200) as per manufacturer's instruction. Briefly, samples were boiled with acetic acid, allowed to react with the reagent to be analyzed by a colorimetric assay. Each sample was then quantified in quadruplicates using the spectrophotometer, and values extrapolated from the glucose standard curve.

Results:

The global glucose uptake in the brain does not show a statistically significant difference between all 3 groups as determined by one way ANOVA analysis because the sample size is too small (Fig. 11). However, there seems to be a ~30% decrease in both groups 1 day post-blast compared to sham-treated rats. This is consistent with vestibulomotor deficits identified in the rotarod test. The small-animal PET imaging facility is currently processing the data in order to have a more detailed regional analysis of changes in glucose uptake into specific brain regions, but these representative images indicate that uptake into thalamic nuclei, hippocampus and cerebellum is reduced. Serum glucose levels were not significantly different between treatment groups (1.54 ± 0.25 mg/ml Variability indicates that an additional 12 rats will be needed for a complete analysis of day 1 post-blast. Another similar set of experiments also will be performed 9 days post-blast with^{18}F-FDG-PET as well as a set of rats imaged 1 and 9 days post-blast with ^{18}F-FMISO, the PET tracer that measures oxidative stress. All experiments will be performed in the presence and absence of ORL1 antagonist treatment.

Tasks 4 and 5: Those brain regions identified by PET imaging will be dissected from brains and tissue homogenized for immunoblotting and ELISA. The areas affected the most appear to be cortex, hippocampus, thalamus and cerebellum – all areas providing sufficient tissue for determining changes in one or more proteins in the RISK cascade or used as a biomarker for apoptotic neuronal or activated glial cells. Some tissue from each region will also be prepared for ELISA to examine levels of protein oxidation. Frozen brains will be thawed and those areas dissected within the next 4-6 weeks for immunoblotting and ELISA and that data analyzed.

Tasks 6-11: **Testing paradigm from task 2 will be repeated until enough rat brains from sham, blast, Noc antagonist and blast + antagonist treated rats have been collected to complete immunocytochemistry and Noc radioimmunoassay (RIA) instead of PET imaging.** Animals will be euthanized at 1 or 9 days post-blast. Half of the animals will receive paraformaldehyde perfusion and brains removed and stored frozen. The brains from the other half of the animals will be quickly put on ice, brain regions dissected and tissue prepared for Noc radioimmunoassay.

Two manuscripts are in preparation. The first will correlate pressure-dependent changes in vestibulomotor function with changes in biomarker expression in cerebellum and cortex (results from tasks1 and 2). The second manuscript will correlate PET imaging with region-specific changes in levels of RISK kinase proteins and biomarkers determined by immunoblotting, ELISA, RIA and cognitive function in the two different blast groups (Head blast 80 psi and Chest blast 45 psi).

SPECIFIC AIM 2:

Methods

Drug Treatment: Cells were incubated in fresh MEM:F12 media containing 0.1% protease free bovine serum albumin and 25 mg/ml bacitracin (BSA/BAC) to prevent Noc degradation and adhesion to the culture dish. ORL1 antagonist, Peptide III/BTD (1 μM or 10 μM), PKC inhibitors chelerythrine chloride (Che; 1 μM) and Gö6976 (3 μM), p38 inhibitor SB202190 (10 μM) or NFκB inhibitor QNZ (3 μM) were added 15 min prior to the addition of OFQ/N. Drug treatments were terminated by rapid washes with ice-cold PBS. In some experiments cells treated with SNP (100 μM) at indicated time points as a control of oxidative stress.

Western Blotting: SHSY-5Y and NG108-15 cells were plated into poly-d-lysine coated dishes and serum starved for 3 hr prior to acute treatments and concurrently during 3, 6, and 24 hr treatments. Treatments were terminated by washing 3 times with cold 1X phosphate buffered saline (PBS) and harvested by incubating 1 hr at 4°C with cell lysis buffer (50mM Tris (pH 7.5), 500 mM NaCl, 50 mM NaF, 10 mM EDTA, 1% Triton X-100, 0.02% sodium azide) containing protease inhibitors (2 mM sodium orthovanadate, 10 μM sodium pyrophosphate, 0.25 mM PMSF, protease cocktail(Santa Cruz Biotechnology)). The post-nuclear fraction was removed by centrifuging samples at 15000*g* for 15 min and then protein was estimated using BCA method.

Samples were boiled at 95°C for 10 min and resolved (20 μg protein) on 8-16% SDS-polyacrylamide gels and electrophoretically transferred onto polyvinylidiene fluoride (PVDF) membranes. Membranes were blocked in 5% non-fat milk. Primary antibodies were incubated overnight and secondaries were incubated for 1 hr at room temperature. Antibodies used are as follows: phospho-ERK 1/2 (1:1000; Cell Signaling #9101S); total ERK 1/2 (1:1000; Cell Signaling #9102); phospho-AKT (1:2000; Cell Signaling #4060S); total AKT (1:1000; Cell Signaling #4691S); phospho-JNK (1:500; Cell Signaling #4671S); total JNK (1:1000; Cell Signaling #9258); phosphor-p38 (1:1000; Cell Signaling #9216S); total p38 (1:1000; 9212); cleaved caspase 3 (1:1000; 9661S); caspase 3 (1:1000; Cell Signaling #9665); goat anti mouse (1:3000; Santa Cruz) or goat anti rabbit (1:2000;Santa Cruz) HRP-conjugated secondary antibodies. Blots were processed using a chemiluminescent reagent (Pierce #32106) and images were captured and analyzed using an Ultralum Omega imaging system and Utraquant software.

Nuclear Extraction: After termination of drug treatment, the nuclear fraction was extracted according to protocol provided with the NE-PER Nuclear and Cytoplasmic Extraction Kit in the presence of protease and phosphatase inhibitors (Pierce).

Electromobility Shift Assay (EMSA): DNA oligonucleotides containing the NFκB or Oct-2 consensus binding site (AGT-TGA-GGG-GAC-TTT-CCC-AGG-C and GGC-CGT-AGC-CAG-CGC-CGC-CGC-GCA-GGA (7), respectively) were synthesized with or without 5' biotin label. Binding reactions were prepared following Pierce LightShift Chemiluminescent EMSA Kit protocol. For competition assay, 200X excess of unlabeled probe was added 20 min prior to the addition of nuclear extract at RT. Samples were resolved by electrophoresis, transferred onto zeta probe blotting membrane and cross-linked under UV light. Biotin-labeled DNA probe was detected using the Pierce Chemiluminescent Nucleic Acid Detection Module. First lane of each blot is the blank (BL: free probe without nuclear extract).

Calcium Phosphate Transfection and Dual-Luciferase Reporter Assay for NFκB Transcriptional Activation: SH-SY5Y cells were transfected using the calcium phosphate method with 1 μg pGL4.74[*hRluc/*TK] DNA Vector (Renilla*;* Promega) and 5 μg pGL4.32[*luc2P/*NF-κB-RE/Hygro] DNA Vector (firefly; Promega). TNFα (10 ng/ml) served as a positive control for NFκB activation. NFκB transcriptional activation was determined with the Promega Dual-Luciferase Reporter Assay System, according to the manufacturer's protocol.

Statistical Analysis: Data was analyzed using one-way ANOVA with Dunnett's Multiple Comparison Test with Graphpad Prism v.5.0 for Windows. Data were considered statistically significant (*) if p< 0.05.

Results

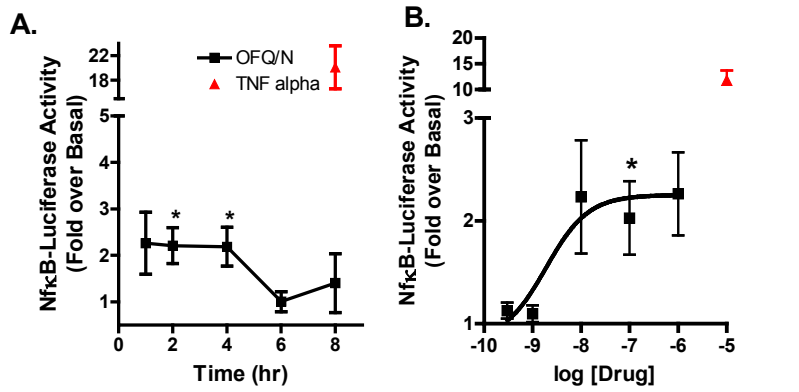

Fig 12. OFQ/N time- and concentration-dependently induces transcriptional activation of NFκB. SH-SY5Y cells were transfected and activity of an NFκB Luciferase dual reporter assay was measured as described. NFκB/Firefly Luciferase activity was normalized to Renilla Luciferase activity and expressed as fold over basal. TNFα, a robust activator of NFκB, served as the positive control. A) OFQ/N treatment (1 μM) increases transcriptional activity of NFκB within 1 hr and B) in a concentration dependent manner (EC_{50} =10 nM). Data expressed as mean ± SEM of 2-11 experiments. (* p<0.05, compared to basal or 300 pM OFQ/N).

Task 1 and Task 2 – NFkB reporter gene activation and analysis of data. Cells were transiently transfected with a reporter gene construct and 24 hr later, activation of the reporter gene by Noc was assessed in SH-SY5Y cells. A time course of activation was determined to plateau by 2 hr and back to baseline by 6 hr (Fig. 11A). The EC_{50} of Noc to activate the reporter gene is 100 nM (Fig. 11B). Similar experiments are underway in NG108-15 cells, as is antagonism of the effect by Noc antagonist to ensure that effects of Noc are mediated through its receptor. However, we have completed EMSA experiments confirming that Noc-mediated binding of NFkB to DNA is blocked by a Noc antagonist (Peptide III BTD), as well as by inhibitors of the NFkB pathway (QNZ) and a RISK cascade protein, PKC (Chelerythrine (Che) and Gö6976 (Go); Fig. 12). However, the p38 inhibitor (SB202190) did not block Noc-mediated NFkB binding to DNA, suggesting that p38 is not involved in Noc-mediated activation of NFkB. This is consistent with a lack of p38 activation seen in the initial immunoblotting experiments in SH-SY5Y cells (Figs 13, 14). Che inhibits all classes of PKC, but Gö6976 inhibits only conventional PKC isoforms. The fact that the Go compound was unable to completely abolish NFkB binding to DNA after Noc treatment suggests that PKC isoforms other than conventional ones are involved in signaling cascades resulting in activation of NFkB. This can be explored further by immunoblotting experiments in both cell lines. Our results clearly indicate that Noc transcriptionally activates NFkB.

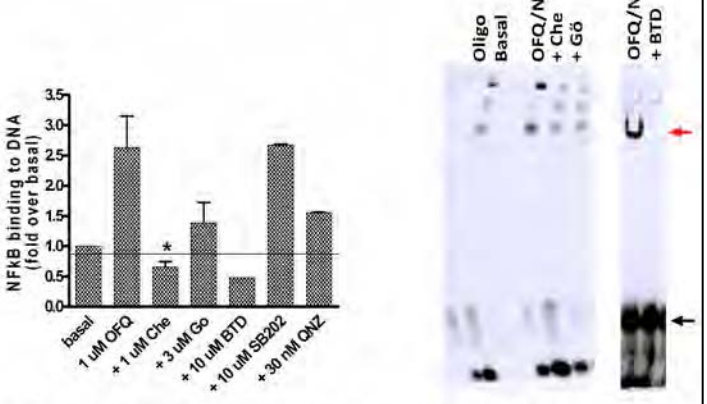

Fig 13. PKC Inhibitors and ORL1 antagonist block OFQ/N-induced NFκB binding. SH-SY5Y cells were treated for 2 hr with 1 μM OFQ/N in the presence or absence of PKC inhibitors Che (1 μM) or Gö6976 (3 μM), p-38 inhibitor SB202190 (10 μM), NFκB inhibitor QNZ (30 nM) or ORL1 antagonist BTD (10 μM). Both PKC inhibitors reduced NFkB binding, as did the ORL1 antagonist BTD. Representative blot and mean densitometric analysis ± SEM of 2-6 experiments are shown.

Tasks 3 and 4 – We have established the time course of activation of RISK cascades following Noc treatment, and included sodium nitroprusside (SNP) as a positive control for RISK cascade activation in both SH-SY5Y and NG108-15 cells (Fig. 14) and begun analysis of data (Fig. 15). It was known from previous reports that Noc acutely activated ERK in SH-SY5Y and NG108-15 cells (Zhang et al., 1999; Thakker and Standifer, 2002), that it activated p38 in NG108-15 cells (Zhang et al., 1999) and that it was capable of activating JNK (Chan et al., 2000), but its ability to activate p38 in SH-SY5Y cells or JNK in both cells, as well as its ability to activate any cascade after prolonged exposure had not been examined. Preliminary studies confirm that Noc activates ERK acutely and transiently in both cell lines, but that ERK activation appears again by 6-24 hr (Figs, 14, 15). Long term activation of JNK is also evident in SH-SY5Y cells. It will be interesting to see how the pieces fall together as the experiments are

repeated in the presence and absence of ORL1 antagonist in both cell lines as there is in vivo evidence linking Noc-mediated activation of ERK and JNK with impaired cerebrovasodilation and hypoxia/ischemia following percussion fluid injury in piglets (Ross and Armstead, 2005).

Fig. 14. Activation of RISK signaling cascades following Nociceptin or SNP treatment.
NG108-15 (A) and SH-SY5Y (B) cells were treated in the absence or presence of Noc (1 μM) or SNP (100 μM; positive control) for indicated time points. Cells were serum starved 3 hr prior to 1, 3, 5, 30 and 60 min treatments and concurrently for 3, 6, and 24 hr treatments. These are representative blots of two experiments.

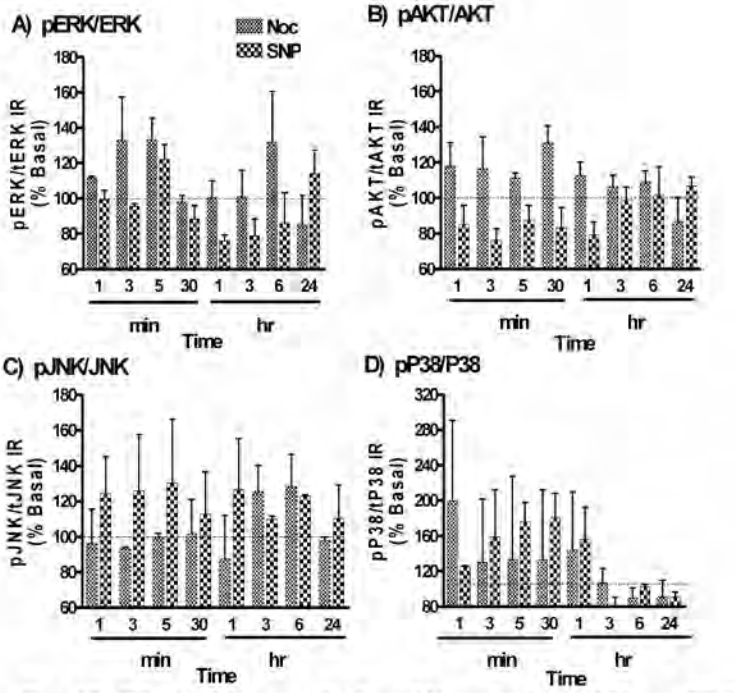

Fig. 15. Effect of Noc or Sodium Nitroprusside (SNP) on RSK cascades in SH-SY5Y cells. Cells were treated for up to 24 hr with Noc (1 μM) or SNP (100μM). Cell lysates were assayed for activation of ERK (A), AKT (B), JNK (C) and P38 (D) by immunoblotting as described in methods. Immunoreactivity was determined by chemiluminescence detection. Values represent mean± SD for n=2.

Tasks 5 and 6: Determine if Noc treatment causes oxidative stress over a 1-24 hr period using a protein carbonyl ELISA approach and analyze data.

These studies were recently initiated and analysis will begin next week.

Task 7: Evaluate cell data and assess if sufficient to write manuscript.

The first manuscript describing Noc activation of NFkB is in preparation and is expected to be ready for submission by the end of September. As the data are compiled and analyzed from tasks 3-6, manuscript preparation will begin. It is anticipated that the first manuscript from those studies will be in preparation in early fall.

Tasks 8 and 9: Measure changes in gene transcription in mRNA dependent kinases upon activation by Noc using qPCR and write manuscript.

There are multiple gene products arising from activation of NFkB and RISK signaling cascades. To avoid trying to determine if there are changes in all of them, we will determine transcription of which genes will be determined after the bulk of the immunoblotting experiments are completed. We routinely employ qPCR in the lab and anticipate no technical problems with this approach using tissue from rat brain. These studies will begin in the fall. There is a single report in a recombinant cell system that Noc binding to ORL1 initiates activation of STAT3 (Wu et al., 2003). This has never been demonstrated with natively expressing receptors, but this is one pathway that will be further explored for signaling and gene transcription possibilities.

KEY RESEARCH ACCOMPLISHMENTS:

- We established that vestibulomotor function in rats is impaired in a pressure-dependent manner after only one day with a head blast threshold of 80 psi. This depression of motor function, balance and coordition is maintained for at least 9 days.
- The decreased vestibulomotor function following bTBI produced no effect on swimming ability or vision as determined by cued navigation in the MWM.
- The 80 psi blast significantly increases reactive astrocyte expression in the cerebellum after 9 days, but not after two days post-blast. This expression is consistent with injury or inflammation and correlates with increased expression of the apoptotic marker, cleaved caspase 3 in the same areas.
- Cleaved caspase 3 expression also is increased in sensory and motor cortices, as well as the neuron axonal injury marker, APP.
- Blast to the head or chest reduces global glucose uptake into the brain, especially in hippocampal and thalamic regions, as determined by uptake of ^{18}F-FDG and PET imaging.
- The neuromodulatory peptide, Noc, that has been implicated in hypoxia/ischemia/reperfusion injury following fluid percussion injury activates gene transcription mediated through NFkB with 10 nM potency and reaches a plateau of activation within 1-2 hr.
- Noc-mediated NFkB DNA binding is blocked by ORL1 antagonists and PKC inhibitors, and is concentration- and time-dependent.

REPORTABLE OUTCOMES:

1. Awwad HO, Gu X, Gonzalez LP, Lerner MR, Tompkins P, Brackett DJ and **Standifer KM** (2010) Blast-induced traumatic brain injury reduces rotarod performance in Sprague-Dawley male rats. Graduate Research Education and Technology Symposium 2010, University of Oklahoma Health Sciences Center, Oklahoma city, OK. Abstract #3. (Hibah won one of three postdoctoral research awards from the Graduate College based upon this poster).

2. Abstracts published and poster presented at Experimental Biology 2010 meeting, Apr 2010 in Anaheim CA:
    a. Awwad HO, Gonzalez LP, Lerner MR, Tompkins P, Brackett DJ and **KM Standifer** (2010) BLAST-INDUCED TRAUMATIC BRAIN INJURY REDUCES ROTAROD PERFORMANCE IN SPRAGUE-DAWLEY MALE RATS. *FASEB J.* 24:811.7
    b. CL Donica, Awwad HO, H Wu and **KM Standifer** (2010) Orphanin FQ/nociceptin activates nuclear factor kappa B in neuronal cells. *FASEB J.* 24:962.13

3. Invited talk at ASPET Neuropharmacology division, as a finalist for Postdoctoral Awards. Hibah O. Awwad was awarded 1st place in postdoctoral contest, and received the ASPET achievement award (attached in APPENDIX) and $500 cash prize.

4. Hibah O. Awwad was also awarded an executive committee membership for a year on ASPET Neuropharmacology division.

CONCLUSIONS:

- Provides a link between reactive gliosis and apoptosis and impaired vestibulomotor function after bTBI.
- Both head and chest blasts impair working memory.
- 80 psi blast-induced TBI depresses motor function, balance and coordination.
- GFAP increase in the cerebellum of blast TBI rats is indicative of reactive astrogliosis, the reactive response by astrocytes to CNS damage.
- Cleaved caspase-3 increase in the cerebellum of blast TBI rats suggests that 80 psi blast triggers pro-apoptotic pathways which further damage the central nervous system.
- Further analysis of different brain sections and brain regions is required to determine the impact of blast TBI on brain regions associated with vestibulomotor function.
- Noc has been noted as having both pro- and anti-inflammatory properties and increased levels of Noc in CSF or plasma are associated with severe pain. While it's not been determined whether Noc increases in response to inflammation, injury or pain or as a result of inflammation, injury or pain, the discovery that Noc increases NFkB binding to DNA and activates transcription helps to explain these varied actions.

Implications:

This is the first report that documents a blast threshold over which vestibulomotor function is depressed. Our results correlate with activation of injury/inflammatory cells and pathways in brain regions associated with vestibulomotor function: the cerebellum and sensory and motor cortices. Though our analysis is not yet complete, evidence suggests that Noc expression is increased in both brain areas as well. While we will continue to study the effects of head and chest blast on cognitive function with the MWM model, we will also pursue the mechanistic basis for the blast-induced vestibulomotor deficit. A more complete understanding of these mechanisms will enable specific treatment that can be administered in the field immediately after a blast to prevent the development of this deficit. Remaining studies will confirm the role of Noc in cognitive and vestibulomotor deficits by administering an ORL1 antagonist intravenously within 1 hr of bTBI to determine if the molecular, biochemical and physical deficits are prevented or reduced.

The determination that Noc activates NFkB also is exciting. Depending on which isoform of NFkB is activated (p50 or p65) and whether homodimers or heterodimers translocate into the nucleus will determine whether NFkB is activating or inhibiting transcription. Since Noc expression is increased so rapidly, it can initiate NFkB signaling quickly to modulate various conditions. By understanding better which downstream effectors of NFkB are modulated by Noc, it will allow us to determine what sort of treatment will be beneficial under what circumstance to prevent these actions.

REFERENCES:

Armstead W. NOC/oFQ activates PKC and generates superoxide to impair hypotensive cerebrovasodilation after hypoxia/ischemia. Med Sci Monit. 2002, 8(1):BR8-BR14.

Armstead WM. Role of NOC/oFQ in impaired opioid-induced pial artery dilation following brain injury. Brain Res. 2000, 869(1-2):231-35.

Armstead, WM. Relationship between nociceptin/orphanin FQ and cerebral hemodynamics after hypoxia-ischemia in piglets. Am J Physiol Heart Circ Physiol. 2000, 278: H477-H483.

Armstead WM. NOC/oFQ contributes tohypoxic-ischemic impairment of N-methyl-D-aspartate-induced cerebral vasodilation. Brain Res. 2000, 868(1):48-55.

Awasthi V, Holter J, Thorp K, Anderson S, Epstein R. F-18-fluorothymidine-PET evaluation of bone marrow transplant in a rat model Nucl Med Commun. 2010, 31(2):152-8.

Bauman RA, Elsayed N, Petras JM, Widholm J. Exposure to sublethal blast overpressure reduces the food intake and exercise performance of rats. Toxicology. 1997, 121(1):65-79.

Belanger HG, Kretzmer T, Yoash-Gantz R, Pickett T, Tupler LA. Cognitive sequelae of blast-related versus other mechanisms of brain trauma. J Int Neuropsychol Soc. 2009, 15(1):1-8.

Cernak I, Savic J, Ignjatovic D, Jevtic M. Blast injury from explosive munitions. J Trauma. 1999, 47(1):96-103; discussion 103-4.

Chan AS, Wong YH. Regulation of c-Jun N-terminal kinase by the ORL(1) receptor through multiple G proteins. J Pharmacol Exp Ther. 2000, 295(3):1094-100.

Courtney AC, Courtney MW. A thoracic mechanism of mild traumatic brain injury due to blast pressure waves. Med Hypotheses. 2009, 72(1):76-83.

Courtney MW, Courtney AC. Working toward exposure thresholds for blast-induced traumatic brain injury: Thoracic and acceleration mechanisms. Neuroimage. 2010, May 17. [Epub ahead of print]

DePalma RG, Burris DG, Champion HR, Hodgson MJ. Blast injuries. N Engl J Med. 2005, 352(13):1335-42.

DeWitt DS, Prough DS. Blast-induced Brain injury and posttraumatic hypotension and hypoxemia. J Neurotrauma. 2009. 26(6):877-87.

Fausti SA, Wilmington DJ, Gallun FJ, Myers PJ, Henry JA. Auditory and vestibular dysfunction associated with blast-related traumatic brain injury. J Rehabil Res Dev. 2009, 46(6):797-810.

Goeldner C, Reiss D, Wichmann J, Meziane H, Kieffer BL, Ouagazzal AM. Nociceptin receptor impairs recognition memory via interaction with NMDA receptor-dependent mitogen-activated protein kinase/extracellular signal-regulated kinase signaling in the hippocampus.J Neurosci. 2008, 28(9):2190-8.

Gottshall KR, Hoffer ME. Tracking recovery of vestibular function in individuals with blast-induced head trauma using vestibular-visual-cognitive interaction tests. J Neurol Phys Ther. 2010, 34(2):94-7

Gross H, Kling A, Henry G, Herndon C, Lavretsky H. Local cerebral glucose metabolism in patients with long-term behavioral and cognitive deficits following mild traumatic brain injury. J Neuropsychiatry and Clinical Neurosci 1996, 8(3):324-34

Hamm RJ. Neurobehavioral Assessment of Outcome following Traumatic Brain Injury in Rats: An Evaluation of Selective Measures. Journal of Neurotrauma, 2001, 18(11): 1207-1216.

Hicks RR, Fertig SJ, Desrocher RE, Koroshetz WJ, Pancrazio JJ. Neurological effects of blast injury. J Trauma. 2010, 68(5):1257-63.

Huckans M, Pavawalla S, Demadura T, Kolessar M, Seelye A, Roost N, Twamley EW, Storzbach D. A pilot study examining effects of group-based Cognitive Strategy Training treatment on self-reported cognitive problems, psychiatric symptoms, functioning, and compensatory strategy use in OIF/OEF combat veterans with persistent mild cognitive disorder and history of traumatic brain injury.J Rehabil Res Dev. 2010, 47(1):43-60.

Irwin RJ, Lerner MR, Bealer JF, Brackett DJ, Tuggle DW. Cardiopulmonary physiology of primary blast injury. J Trauma. 1997, 43(4):650-5.

Irwin RJ, Lerner MR, Bealer JF, Lightfoot SA, Brackett DJ and Tuggle DW. Global primary blast injury: a rat model. Journal of Oklahoma State Medical Association, 1998, 91(7): 387-392

Jaffee MS et al, J Rehabil Res Dev 2009, Jaffee MS, Helmick KM, Girard PD, Meyer KS, Dinegar K, George K. Acute clinical care and care coordination for traumatic brain injury within Department of Defense J Rehabil Res Dev. 2009, 46(6):655-66.

Lehr HA, van der Loos CM, Teeling P and Gown AM. Complete Chromagen Separation and Analysis in Double Immunohistochemical Stains Using Photoshop-based Image Analysis. The Journal of Histochemistry and Cytochemistry 1999, 47(1): 119-125.

Leung LY, VandeVord PJ, Dal Cengio AL, Bir C, Yang KH, King AI. Blast related neurotrauma: A review of cellular injury. Mol Cell Biomech, 2008, 5:155-168

Ling G, Bandak F, Armonda R, Grant G, Ecklund J. Explosive blast neurotrauma. J Neurotrauma. 2009, 26(6):815-25.

Long JB, Bentley TL, Wessner KA, Cerone C, Sweeney S, Bauman RA. Blast overpressure in rats: recreating a battlefield injury in the laboratory. J Neurotrauma. 2009, 26(6):827-40.

Mandolesi L, Leggio MG, Graziano A, Neri P, Petrosini L. Cerebellar contribution to spatial event processing: involvement in procedural and working memory components. Eur J Neurosci. 2001, 14(12):2011-22.

Mandyam CD, Thakker DR, Christensen JL, Standifer KM. Orphanin FQ/nociceptin-mediated desensitization of opioid receptor-like 1 receptor and mu opioid receptors involves protein kinase C: a molecular mechanism for heterologous cross-talk. J Pharmacol Exp Ther. 2002, 302(2):502-9.

Peskind ER, Petrie EC, Cross DJ, Pagulayan K, McCraw K, Hoff D, Hart K, Yu CE, Raskind MA, Cook DG, Minoshima S. Cerebrocerebellar hypometabolism associated with repetitive blast exposure mild traumatic brain injury in 12 Iraq war Veterans with persistent post-concussive symptoms. Neuroimage. 2010, Apr 10. [Epub ahead of print]

Petras JM, Bauman RA, Elsayed NM. Visual system degeneration induced by blast overpressure. Toxicology. 1997, 121(1):41-9.

Risling M, Plantman S, Angeria M, Rostami E, Bellander BM, Kirkegaard M, Arborelius U, Davidsson Mechanisms of blast induced brain injuries, experimental studies in rats. J. Neuroimage. 2010 May 21. [Epub ahead of print]

Rosenfeld JV, Ford NL. Bomb blast, mild traumatic brain injury and psychiatric morbidity: a review.Injury. 2010, 41(5):437-43.

Ross J and Armstead WM. NOC/oFQ activates ERK and JNK but not p38 MAPK to impair prostaglandin cerebrovasodilation after brain injury. Brain Res. 2005, 1054(1):95-102.

Säljö A, Bolouri H, Mayorga M, Svensson B, Hamberger A. Low-level blast raises intracranial pressure and impairs cognitive function in rats: prophylaxis with processed cereal feed. J Neurotrauma. 2010, 27(2):383-9

Saljo et al, Neuroimage 2010, Säljö A, Mayorga M, Bolouri H, Svensson B, Hamberger A. Mechanisms and Pathophysiology of the Low-level Blast Brain Injury in Animal Models. Neuroimage. 2010 May 21. [Epub ahead of print]

Scherer MR, Schubert MC. Traumatic brain injury and vestibular pathology as a comorbidity after blast exposure Phys Ther. 2009, 89(9):980-92.

Svetlov SI, Larner SF, Kirk DR, Atkinson J, Hayes RL, Wang KK. Biomarkers of blast-induced neurotrauma: profiling molecular and cellular mechanisms of blast brain injury J Neurotrauma. 2009, 26(6):913-21.

Svetlov SI, Prima V, Kirk DR, Gutierrez H, Curley KC, Hayes RL, Wang KK. Morphologic and Biochemical Characterization of Brain Injury in a Model of Controlled Blast Overpressure ExposureJ Trauma. 2010 Mar 2. [Epub ahead of print]

Vasterling JJ, Verfaellie M, Sullivan KD. Mild traumatic brain injury and posttraumatic stress disorder in returning veterans: perspectives from cognitive neuroscience Clin Psychol Rev. 2009, 29(8):674-84.

Vorhees CV, Williams MT. Morris water maze: procedures for assessing spatial and related forms of learning and memory. Nat Protoc. 2006, 1(2):848-58.

Witta J, Buzas B, Cox BM (2003) Traumatic brain injury induces nocieptin/orphanin FQ expression in neurons of the rat cerebral cortex. Neurotrauma. 2003, 20(6):523-32

Wu EH, Lo RK, Wong YH. Regulation of STAT3 activity by G16-coupled receptors. Biochem Biophys Res Commun. 2003, 303(3):920-5.

Zhang Z, Xin SM, Wu GX, Zhang WB, Ma L, Pei G. Endogenous delta-opioid and ORL1 receptors couple to phosphorylation and activation of p38 MAPK in NG108-15 cells and this is regulated by protein kinase A and protein kinase C. J Neurochem. 1999, 73(4):1502-9.

APPENDICES:

1. ASPET achievement award
2. Copy of Abstract for OUHSC GREAT 2010
3. Copy of Abstracts for EB 2010 and the ASPET scientific program.
4. Copy of OUHSC award winners
5. Irwin RJ, Lerner MR, Bealer JF, Lightfoot SA, Brackett DJ and Tuggle DW. Global primary blast injury: a rat model. Journal of Oklahoma State Medical Association (1998) vol 91(7): 387-392.
6. MWM protocol (Vorhees and Williams, 2006)

SUPPORTING DATA:

Full size Fig. 11 – FDG-PET imaging.

Full size Fig. 14 - NG108-15 and SH-SY5Y immunoblots

The Division for Neuropharmacology

of

The American Society for Pharmacology and Experimental Therapeutics

Postdoctoral Young Scientist Award

First Place Winner

Hibah Awwad

University of Oklahoma Health Sciences Center

aspet 100 YEARS 1908–2008

Experimental Biology 2010
Anaheim, CA
April 24-28, 2010

35th Annual Graduate Research Symposium

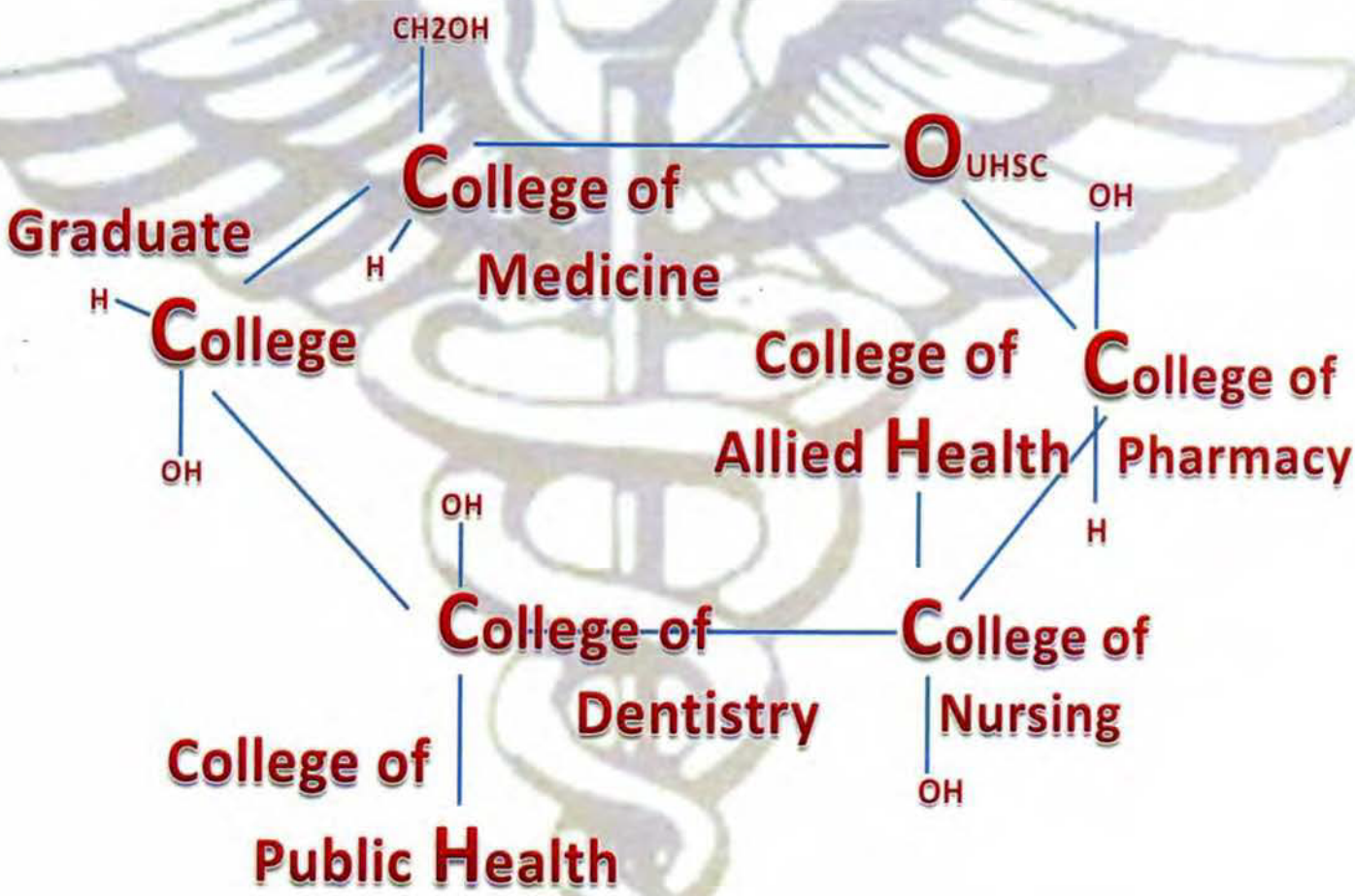

March 29 - April 1, 2010

Sponsored by:

Graduate Student Association and Graduate College

I.
Schedule of Events

****Monday, March 29, 2010****

8:00 am-9:00 am
Postdoctoral Fellow Poster Set Up
Robert M. Bird Library Foyer

9:00 am-11:00 am
Postdoctoral Fellow Poster Judging
Robert M. Bird Library Foyer

9:30-11:00
Professional Student Oral Presentation Competition
Robert M. Bird Library Auditorium, Room 299

11:00 am-1:00 pm
Postdoctoral Fellow Poster Viewing
Robert M. Bird Library Foyer

4:00pm-5:00pm
Postdoctoral Fellow Poster Removal

****Tuesday, March 30, 2010****

8:00 am-12:00 pm
Oral Presentation Competition
Robert M. Bird Library Auditorium Room 299
Biomedical Research Center, Room 109

9:00 am-10:00 am
Graduate, Professional,& OSSM Student Poster Set Up
Robert M. Bird Library Foyer

12:00 pm-1:00 pm
Luncheon for Presenters and Attendees
Robert M. Bird Library Foyer

****Tuesday March 30, 2010****

continued

II.
POSTDOCTORAL RESEARCH FELLOW PRESENTATIONS

ABSTRACT #3

BLAST-INDUCED TRAUMATIC BRAIN INJURY REDUCES ROTAROD PERFORMANCE IN SPRAGUE-DAWLEY MALE RATS

Hibah O. Awwad[1], Xiaowu Gu[2], Larry P. Gonzalez[3], Megan Lerner[4], Paul Tompkins[5], Daniel J. Brackett[4] and Kelly M. Standifer[1,2]

[1]Department of Pharmaceutical Sciences, [2]Oklahoma Center for Neuroscience, [3]Department of Psychiatry & Behavioral Sciences, [4]Department of Surgery & VA Medical Center, [5]Department of Neurosurgery, University of Oklahoma Health Sciences Center, Oklahoma City, OK 73117

Blast-induced traumatic brain injury (bTBI) is the most common injury of modern warfare. In 2008, nearly 25,000 U.S. soldiers were diagnosed with TBI, where neuronal and behavioral defects are detected up to one year post-blast. Research is only beginning to reveal the mechanisms of bTBI. Our objective was to determine the effect of our bTBI model on motor function in rats using the rotarod. Non-blast TBI studies indicate that rotarod is the most sensitive vestibulomotor test, such that it detects deficits even when beam balance and beam walk assays indicate the animal has recovered. Sprague-Dawley male rats (n=7-9/group) were trained on the rotarod apparatus prior to blast injury then tested on days 1-4, 7 and 8 post-blast. On day 9 post-blast, brains were fixed and paraffin-embedded for immunohistochemistry. bTBI was induced by a blast-pressure wave generator, with pressure exposures at ~60 and ~80 psi. Rotarod performance on days 1, 2, 7 and 8 post-blast in 80 psi blast-injured rats was significantly reduced compared to sham rats, whereas 60 psi blast did not reduce rotarod performance. Cerebellar immunoreactivity of the glial fibrillary acidic protein (GFAP), a marker for reactive astrocytes, was significantly increased in rats that received an 80 psi blast compared to sham rats. Our results indicate a direct link between blast-induced brain injury and an increase in reactive astrocytes in the cerebellum. This is the first study, to our knowledge, to show a pressure-dependent effect on rotarod performance as a measure of vestibulomotor function in bTBI.

Funding
This work was supported by Department of Defense (CDMRP) – grant DR080343

GREAT Winners 2010

Name	Award	Department	Mentor
Aaron McLain	COM GSA Travel Grant	Biochemistry and Molecular Biology	Like Szweda, PhD
Abigail Smith	ORA Award for Outstanding Research	Microbiology and Immunology	John West, PhD
Beverly Crider	GPiBS Anniversary Award	Cell Biology	James J. Tomasek, PhD
Candace Robledo	GSA Award for Outstanding Research	Biostatistics and Epidemiology	Jennifer Peck, PhD
Carl Grafe	Graduate College Travel Award	Biostatistics and Epidemiology	Aaron Wendelboe, PhD
Chaoyong He, PhD	Postdoctoral Fellow Travel Award	Endocrinology	Zhonglin Xie, PhD
Charlotte Chung	Graduate College Dean's Award for Outstanding Research Travel Award	Neuroscience	Jordan Tang, PhD
Christopher Conrady	College of Medicine Travel Award	Microbiology and Immunology	Daniel J. Carr, PhD
Courtney Long	Keynote Speaker Travel Award	Microbiology and Immunology	Mary Beth Humphrey, MD, PhD
E-Ching Ong	College of Medicine Dean's Award for Outstanding Research Travel Award	Cell Biology	Leonidas Tsiokas, PhD
E-Ching Ong	COM GSA Travel Grant	Cell Biology	Leonidas Tsiokas, PhD
E-Ching Ong	GSA Travel Grant	Cell Biology	Leonidas Tsiokas, PhD
Erin Davis	Graduate College Travel Award	Biostatistics and Epidemiology	Barbara Neas, PhD
George Malantinszky	Outstanding High School Research	OSSM	Jens Kreth, PhD
George Risinger, PhD	Postdoctoral Fellow Travel Award	Cell Biology	James J. Tomasek, PhD
Hibah Awwad, PhD	Postdoctoral Fellow Travel Award	Pharmaceutical Sciences	Kelly Standifer, PhD
Jordi Lanis	GSA Travel Grant	Microbiology and Immunology	Jimmy Ballard, PhD
Kathleen Cooley	OMRF Travel Award	Biochemistry and Molecular Biology	Jordan Tang, PhD
Lisa Zhang	Outstanding High School Research	OSSM	A.K. Fazlur Rahman
Mandi Wiley	Provost's Award for Outstanding Research	Microbiology and Immunology	Ira Blader, PhD
Oriana Hawkins	Oklahoma BioScience Travel Award	Microbiology and Immunology	William Hildebrand, PhD
Pascal Nitiema	Sigma Xi Travel Award	Biostatistics and Epidemiology	Helene Carabin, PhD
Randy Hempel	Career Development Speaker Travel Award	Microbiology and Immunology	Terrence Stull, MD
Ryan Webb	College of Public Health Professional Award	Biostatistics and Epidemiology	Amr Sawalha, MD
Todd Wuest	Graduate College Travel Award	Microbiology and Immunology	Daniel J. Carr, PhD
Vivek Gupta, PhD	Postdoctoral Fellow Travel Award	Cell Biology	Raju Rajala, PhD

The FASEB Journal
AVANTI FOR Avanti POLAR LIPIDS, INC.
QUICK SEARCH: [advanced]
Author: Keyword(s):
Go Awwad
HOME HELP FEEDBACK SUBSCRIPTIONS ARCHIVE SEARCH SEARCH RESULT
Year: Vol: 24 Page:

Selected Abstracts

Download ALL Selected Citations to Citation Manager

Returned: 2 citations and abstracts. **Click on down arrow or scroll to see abstracts.**

Hibah Omar Awwad, Larry P Gonzalez, Megan R. Lerner, Paul Tompkins, Daniel J Brackett, and Kelly M Standifer
Blast-induced traumatic brain injury reduces rotarod performance in Sprague-Dawley male rats
FASEB J. 24: 811.7

Courtney L Donica, Hibah O Awwad, Huaqing Wu, and Kelly M Standifer
Orphanin FQ/Nociceptin Activates Nuclear Factor Kappa B In Neuronal Cells
FASEB J. 24: 962.13

Abstract 1 of 2

811.7

Blast-induced traumatic brain injury reduces rotarod performance in Sprague-Dawley male rats

Hibah Omar Awwad[1], Larry P Gonzalez[2], Megan R. Lerner[3], Paul Tompkins[4], Daniel J Brackett[3] and Kelly M Standifer[1]

[1] Department of Pharmaceutical Sciences
[2] Department of Psychiatry & Behavioral Sciences
[3] Department of Surgery & VA Medical Center
[4] Department of Neurosurgery, University of Oklahoma Health Sciences Center, Oklahoma City, OK

ABSTRACT

Blast-induced traumatic brain injury (bTBI) is the most common injury of modern warfare. In 2008, nearly 25,000 U.S. soldiers were diagnosed with TBI, with neuronal and behavioral defects detected up to one year post-blast. Research is only beginning to reveal the mechanisms of bTBI. Our objective was to determine the effect of our bTBI model on motor function in rats using the rotarod. Non-blast TBI studies assure the high sensitivity of the rotarod as a vestibulomotor test, where deficits are detected even after recovery from beam balance/walk. Sprague-Dawley male rats pretrained on the rotarod apparatus prior to blast injury were tested on days 1–4, 7 and 8 post-blast. bTBI was induced by a blast-pressure wave generator, with exposures at ~60 and ~80 psi. Rotarod performance on days 1, 2, 7 and 8 post-blast in 80 psi blast-injured rats was significantly reduced compared to sham rats, whereas 60 psi blast did not reduce performance. Cerebellar immunoreactivity of the glial fibrillary acidic protein, a reactive astrocyte marker, was significantly increased on day 9 post-blast in rats exposed to 80 psi blast compared to sham rats. This indicates a direct link between bTBI and increased reactive astrocytes in the cerebellum. This is the first study, to our knowledge, to show a pressure-dependent effect on rotarod performance as a measure of vestibulomotor function in bTBI. Supported by Department of Defense (CDMRP) – DR080343

Abstract 2 of 2

962.13

Orphanin FQ/Nociceptin Activates Nuclear Factor Kappa B In Neuronal Cells

Courtney L Donica[1], Hibah O Awwad[2], Huaqing Wu[2] and Kelly M Standifer[1,2]

[1] Oklahoma Center for Neuroscience

[2] Pharmaceutical Sciences, University of Oklahoma Health Science Center, Oklahoma City, OK

ABSTRACT

Endogenous neuropeptide orphanin FQ/nociceptin (OFQ/N) and its receptor, opioid receptor like-1 (ORL1; or Nociceptin orphanin peptide receptor, NOP), have been shown to play a modulatory role throughout the body on nociceptive sensitivity, including motor function, spatial learning, smooth muscle tone, cardiac function and the immune system. ORL1 is a G protein coupled receptor (GPCR) that couples to Gi/o proteins and modulates expression and release of inflammatory mediators from immune cells and in the CNS. Inhibitory GPCRs have been shown to activate the immune system regulator, NF B. The NF B family consists of several subunits, including p105 and p50. When activated, NF B translocates to the nucleus and can modify transcription. To determine if OFQ/N modulates NF B activity, SH-SY5Y human neuroblastoma cells were treated with OFQ/N and assessed for changes in nuclear accumulation, DNA binding and protein expression. OFQ/N increases the nuclear accumulation of NF B at 30 min and increases the DNA binding of NF B by 1 hr as determined by electromobility shift assay (EMSA). Additionally, immunoblot analysis of SH-SY5Y cell lysates indicates that NF B p50 protein expression is up-regulated by 2 hr. This suggests that OFQ/N may modulate immune system function by activating NF B. These studies were supported by DA017380 and OCAST grant HR08-152 to KMS.

Copyright © 2010 by The Federation of American Societies for Experimental Biology.

Global Primary Blast Injury: A Rat Model

Randy J. Irwin, MD; Megan R. Lerner; John F. Bealer, MD; Stan A. Lightfoot, MD; Daniel J. Brackett; David W. Tuggle, MD

Blast wave injury from bombs cause a unique but poorly understood spectrum of injuries. Previous blast wave models involved high energy explosives detonated in an open field without the sophisticated monitoring of laboratory equipment. We characterized a rodent model that produces a global blast injury in a safe laboratory environment. Male rats, prospectively randomized to four groups of ten, were anesthetized and subjected to a blast at 2.0 cm, 2.5 cm, or 3.5 cm from the blast nozzle. The control group received no blast. Intensity of the blast (80-120 psi peak pressure, 1-2 msec duration) was controlled by varying the distance of the blast wave generator to the rat. The rats were monitored for three hours following the blast and then euthanized. Bradycardia was an immediate but transient response to blast injury. Mean arterial pressure was bimodal with severe hypotension occurring immediately after the blast and, again, two to three hours later. The characteristic injuries from a blast wave, such as pulmonary hemorrhage with increased lung weight, intestinal serosal hemorrhage, and hemoperitoneum, were found in the rats subjected to the blast pressure wave. In conclusion, our rodent model accurately reproduces the clinical spectrum of injuries seen in blast victims and will provide a powerful tool for studying the pathophysiology and potential treatments of bomb blast victims.

Introduction

The increased use of explosives by terrorists has made the management of blast injured victims a problem for civilian, as well as military physicians. An explosive is any substance or device capable of a sudden expansion of a gas, which upon release of its potential energy creates a pressure wave.[1] Based on the mechanism of energy release, explosives are categorized as chemical, mechanical, or atomic. Chemical explosives decompose into a gas upon detonation, and their destructive power is partially dependent upon the rate of decomposition. Low energy chemical explosives such as black powder (potassium nitrate, sulfur, charcoal) burn or deflagrate slowly developing low pressures; whereas high energy chemical explosives such as trinitrotoluene (TNT) detonate at high speeds developing high pressures.[1] Mechanical explosives usually involve a device that confines a compressed gas with a diaphragm. When the pressure of the compressed gas exceeds the burst strength of the diaphragm, an explosion is created. Atomic explosives derive their energy from the disintegration of an atom's nucleus.

The pressure generated from an explosion is transmitted into the surrounding environment as a radially propagating pressure wave that can attain supersonic speeds.[2] When measured, a blast pressure wave has a short positive phase that almost instantaneously rises to its peak pressure, decays over time (Friedlander waves), and ends with a negative pressure or subatmospheric vacuum.[3,4] The area under the curve, the impulse, is proportional to its biologic effect.[4]

Studying the physiologic effects of a blast wave in a clinically useful and scientific model has been difficult because previous models typically used high energy explosives such as trinitrotoluene detonated in an open field or in shock tubes. These blast models are dangerous and lack reproducibility, close observation, and the use of sensitive laboratory equipment. The objective of this study was to develop a reproducible mechanical explosive that simulates

Direct correspondence to: David W. Tuggle, MD, Department of Pediatric Surgery, 940 NE 13, Room 2403, Oklahoma City, Oklahoma 73190.

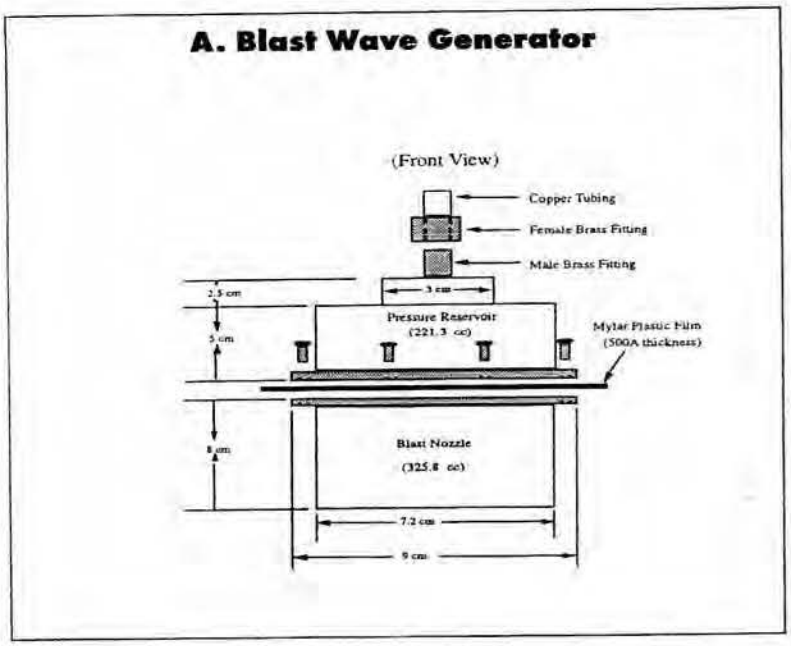

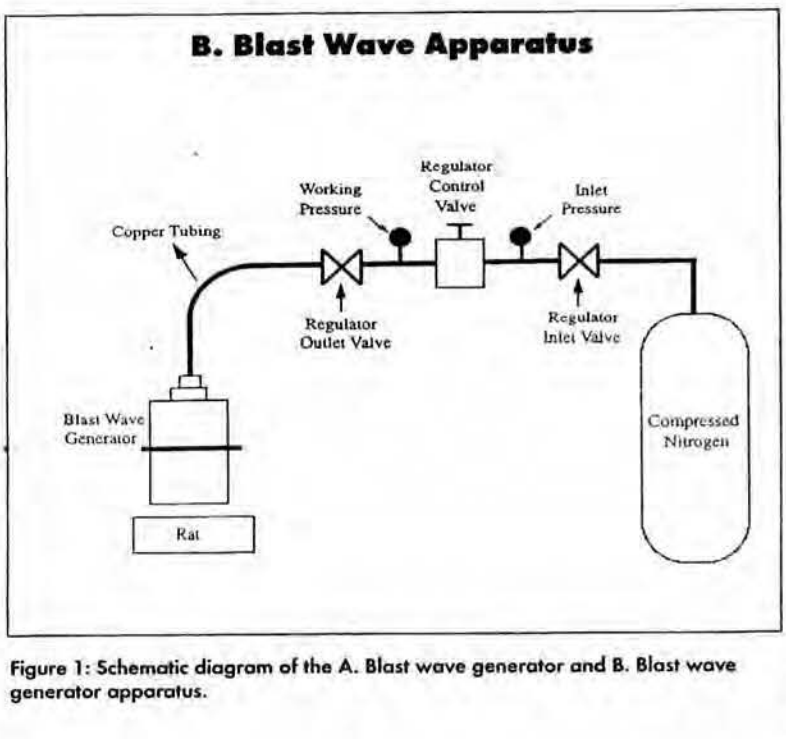

Figure 1: Schematic diagram of the A. Blast wave generator and B. Blast wave generator apparatus.

blast pressure waves from high energy explosives and produces the types of injuries commonly seen in blast injured victims.

Materials and Methods

Blast wave generator:

A blast wave generator was designed and constructed to deliver a global blast pressure wave in a safe laboratory setting. Our blast wave generator (Fig. 1A) consists of three parts: a pressure reservoir, a blast nozzle, and a 500 angstrom Mylar® polyester film (DuPont Films, Wilmington, DE) that separates the two compartments. Compressed nitrogen from a storage tank is slowly delivered by copper tubing under the control of a regulator to charge the pressure reservoir (Fig. 1B). When the pressure in the reservoir exceeds the burst strength of the Mylar® diaphragm, a blast pressure wave is discharged toward the rat by the blast nozzle. All blast waves in this study were measured using an Omega PX603 high frequency air pressure transducer (Omega Engineering Co., Stanford, CT) and analyzed on a Phillips PM 3394 digital oscilloscope (Fluke Electronics Co., Everett, WA) for wave form, peak pressure, and duration.

Animal studies:

This study was approved by the Animal Care and Use Committee at the University of Oklahoma with all animals being handled according to NIH guidelines for the compassionate use of laboratory animals. Forty male, Sprague-Dawley rats (Harlan, Indianapolis, IN) were acclimated and given unlimited access to food and water prior to the experiment. Rats were anesthetized in a bell jar using 5 percent isoflurane in O_2:N_2, 25:75 percent mixture, intubated, weighed, and connected to a Harvard rodent respirator delivering 1.4 percent isoflurane in O_2:N_2, 25:75 percent, mixture with a tidal volume of 12 ml/kg at a rate of 72 bpm. The animals were placed in a supine position on an Aquamatic K20 circulating heating pad (GRI Medical Products, Bellville, OH) to maintain core body temperature. The tip of a PE50 catheter inserted through the left femoral artery was advanced into the abdominal aorta and connected to a Gould pressure transducer for measurement of arterial blood pressure. Heart rate was determined from the arterial pressure tracing.

Three groups of ten rats were subjected to a blast pressure wave centered on the xiphoid with the tip of the blast nozzle located at either 2.0, 2.5, or 3.5 cm from the sternum. Immediately before each blast, the rats were

temporarily taken off the ventilator. Control animals were subjected to the same experimental protocol but did not receive a blast. After an initial baseline reading, mean arterial pressure and heart rate were measured every fifteen minutes for the first hour and every thirty minutes thereafter. Death was defined as a mean arterial pressure less than 30 mmHg for greater than 15 minutes.

Pathologic evaluation:
After three hours, all survivors were euthanized while under anesthesia and necropsy was performed. Gross inspections for typical pathologic findings associated with blast wave injury, such as pulmonary hemorrhage, air emboli, hemoperitoneum, and intestinal serosal hemorrhage, were recorded. The intestines were examined macroscopically for areas of focal hemorrhage using a five-point scale (0 = clear, without evidence of hemorrhage, 1 = light, petechial hemorrhage, 2 = petechial hemorrhage in a banding pattern, 3 = light hemorrhagic banding, and 4 = heavy hemorrhagic banding). The intestines were removed and fixed in 5 percent formalin for histological study using the "Swiss roll" method.[5] The lungs were excised en-bloc, cleaned of extraneous tissue, weighed, and infused intratracheally with 5 percent formalin. Sections of liver, heart, brain, and kidney were fixed in 5 percent formalin. All tissues were paraffin embedded and examined by light microscopy. Pulmonary hemorrhage and edema was quantitated using the lung weight to body weight ratio.[6]

Statistical analysis:
Heart rate and mean arterial pressure were analyzed using a repeated-measures analysis of variance (ANOVA). Post-hoc individual time comparisons were made using Duncan's new multiple range test. Mortality and hemoperitoneum were assessed using Chi-square. Lung wt/body wt ratio and body wt were compared using Student's unpaired *t*-test. The nonparametric median test was used to analyze the intestinal pathology scores. Differences were considered to be significant when the probability level for a chance result was less than 0.05.

Results

Body weight was not statistically significant between the groups (Table 1). Mortality was 60 percent in the 2.0 cm group, all of which died in the first hour (Table 1). All other rats survived the duration of the study.

Table 1. Selected Results from Exposure to Graded Blast Waves

	Weight (grams)	Intestinal score	Hemoperitoneum	Mortality
control	325 ± 11	0 ± 0	0/10	0/10
3.5 cm	323 ± 7	0 ± 0	2/10	0/10
2.5 cm	321 ± 7	1.0 ± 0.4	4/10	0/10
2.0 cm	332 ± 6	0.8 ± 0.5	6/10*	6/10*

Data are mean ± SEM. *p≤0.05 vs. control.

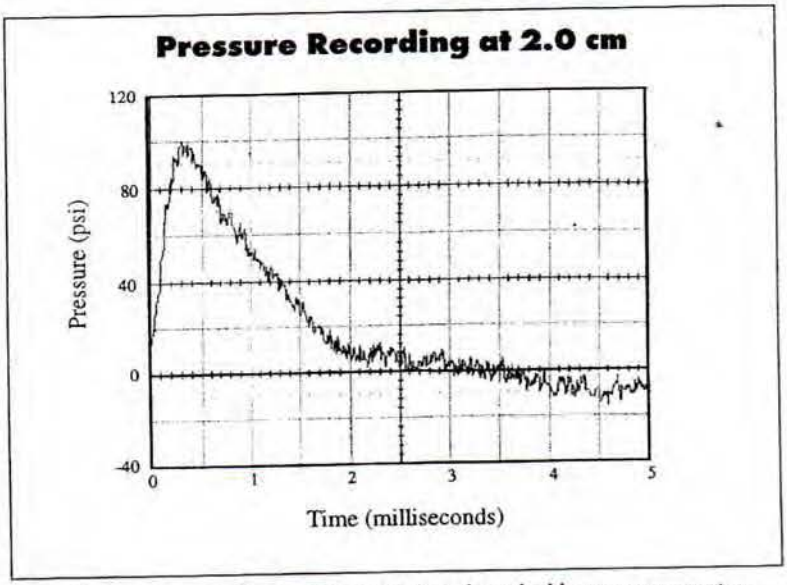

Figure 2: Pressure recording over time at 2.0 cm from the blast wave generator.

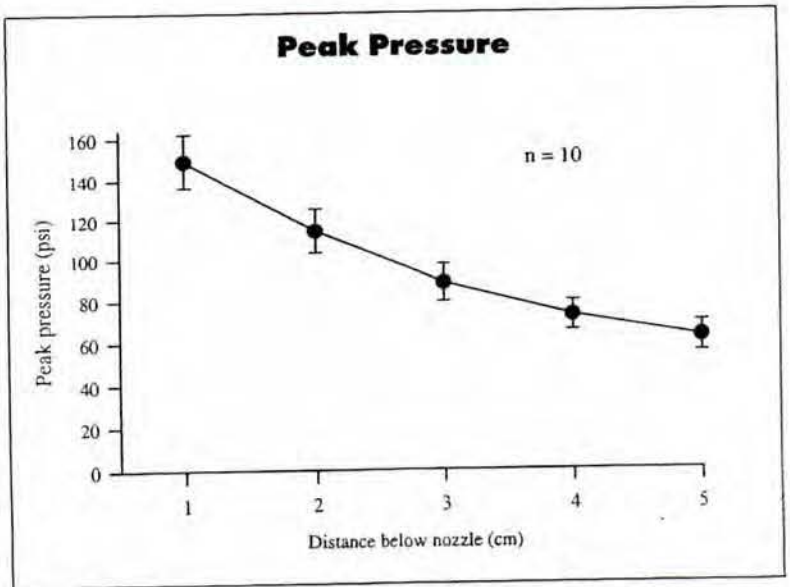

Figure 3: Peak overpressure measured at varying distances from the blast wave generator

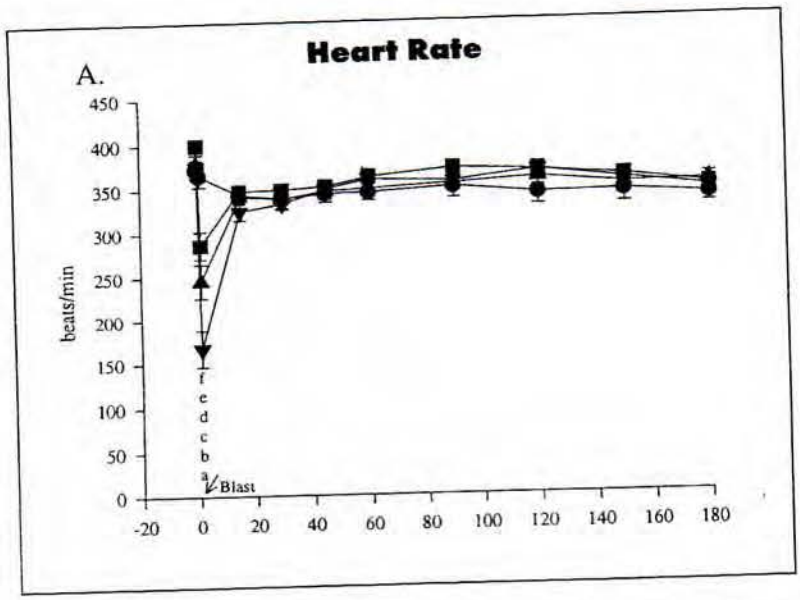

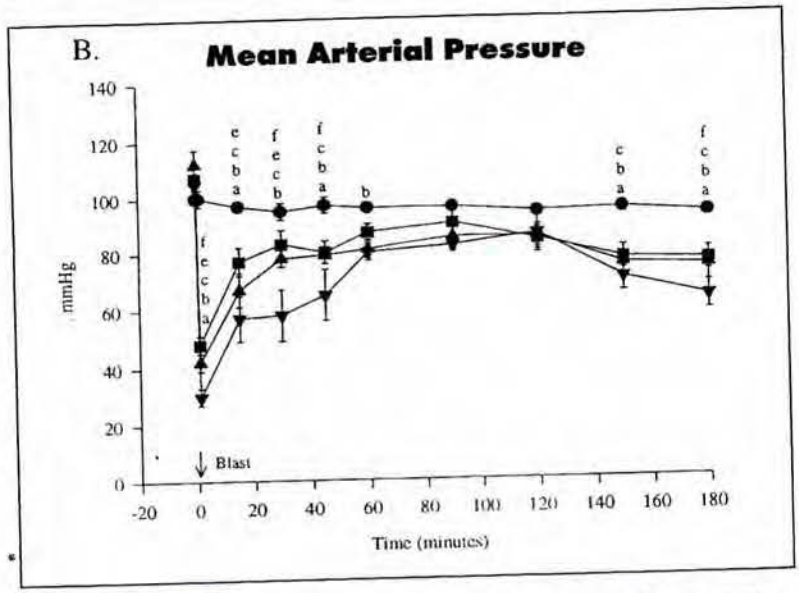

Figure 4: The effects of blast pressure waves on A. Heart rate and B. Mean aortic blood pressure. Symbols representing each group are as follows: ● Control group; ■ 3.5 cm group; ▲ 2.5 cm group; and ▼ 2.0 cm group. Statistically significant differences ($p<.05$) are denoted by: a, Control vs 3.5 cm; b, Control vs 2.5 cm; c, Control vs 2.0 cm; d, 3.5 cm vs 2.5 cm; e, 3.5 cm vs 2.0 cm; f, 2.5 cm vs 2.0 cm.

Blast wave generator:
Pressure curves over time from our blast wave generator revealed a near instantaneous 100 percent rise time (<0.4 msec) to the peak pressure, duration of 1.5 to 3 msec, and a negative phase or suction (Fig. 2). The peak pressure decayed rapidly as it expanded from the blast wave generator (Fig. 3), allowing rats exposure to different blast intensities by simply varying the distance between the blast wave generator and the rat.

Hemodynamics:
The animals developed severe bradycardia immediately after the blast that was only transient in nature with a return to control values within fifteen minutes (Fig. 4A). Within seconds of the blast wave, the animals developed profound hypotension to less than 50 percent of control levels (Fig. 4B). Over time, the survivors' mean arterial pressure slowly recovered but never reached preblast levels. After two hours the rats, again, became significantly hypotensive when compared to controls.

Pathology:
At autopsy, no rats showed external signs of injury. Internally, tissue damage occurred mostly to air containing organs such as the lungs and intestines. The most frequent and obvious injury was bilateral pulmonary hemorrhage occurring mostly in the lower lobes near the diaphragm and medially near the mediastinum. Microscopically (Fig. 5) the blasted rats' lungs showed characteristic signs of blast injury such as disruption of the alveolar parenchyma and capillaries with exudation of blood and fluid into the interstitial and alveolar spaces.[7,8] Pulmonary injury, quantitated by lung wt/body wt ratio, increased with higher intensity blasts signifying increased pulmonary hemorrhage and edema. (Fig. 6) Air emboli were seen grossly in the left ventricle of the heart and large arteries of a few animals blasted at 2.0 cm and histologically in the bronchial and cerebral arteries. Air emboli were not seen in the control animals or venous circulation of the blasted animals.

Gross examination of the intestines showed a variety of lesions from punctate hemorrhages to discrete annular hemorrhagic bands with intramural hematoma although not statistically significant between groups (Table 1). Light microscopy revealed subserosal hemorrhage and focal areas of necrosis with sloughing of the crypts and villi (Fig. 7).

Microscopic examination of the heart showed evidence of myocardial contusion. Hemoperitoneum, presumably from fracture of the liver, occurred more frequently in higher intensity blasts (Table 1). The kidneys of our blasted rats contained microscopic hemorrhage most frequently at the medullary-cortex junction.

Discussion

The damage inflicted on the human body by bomb blasts is mediated by three different mechanisms. Primary blast injury, which is the focus of this study, results from the impact of the blast wave on the body. Secondary blast injury is caused by tissue penetration of flying debris created by the blast pressure wave.[2] Tertiary blast injury occurs from collapsing buildings or the result of the body being violently thrown. Primary blast injury can occur by itself or, more commonly, in conjunction with secondary or tertiary injuries. Primary blast injury inflicts a unique form of trauma without external signs of injury causing it to be easily overlooked in mass casualty situations. To study this unique form of trauma required the development of a new model that is reproducible, safe, and allows for physiologic monitoring.

Blast wave generator:

Our blast pressure waves were reproducible and identical in form to blast waves from high energy explosives such as trinitrotoluene,[1,9] allowing the study of blast injuries in a safe laboratory setting. The peak pressure from our blast wave generator could be easily increased or decreased by simply changing the distance between the blast wave generator and the rat.

Hemodynamics:

The immediate, transient bradycardia that we witnessed has been attributed to a vagal reflex.[10] Hypotension after a blast injury has been measured by some investigators[10,11] and is believed to result from myocardial ischemia from air emboli to the coronary arteries or cor pulmonale, but the etiology remains unproven.

Pathology:

Injuries occurred most commonly in gas containing organs such as the lung and intestines. The pathognomonic sign of blast wave injury is pulmonary hemorrhage and edema, sometimes called "blast lung." Blast injuries disrupt the alveolar parenchyma and capillaries causing hemorrhage and edema by two mechanisms:

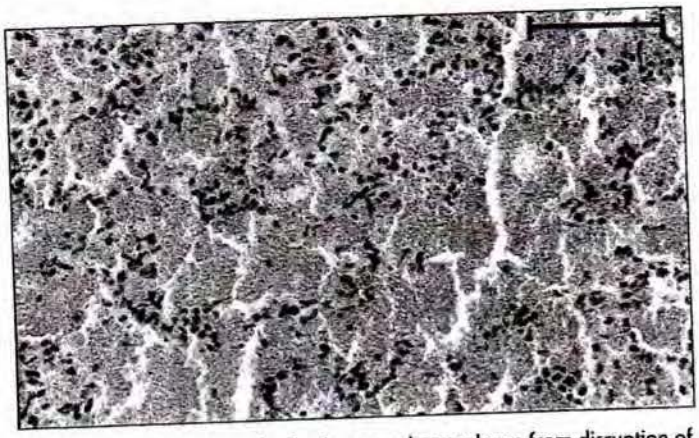

Figure 5: Photomicrograph of pulmonary hemorrhage from disruption of the alveolar septa and capillaries. Bar = 0.5 mm.

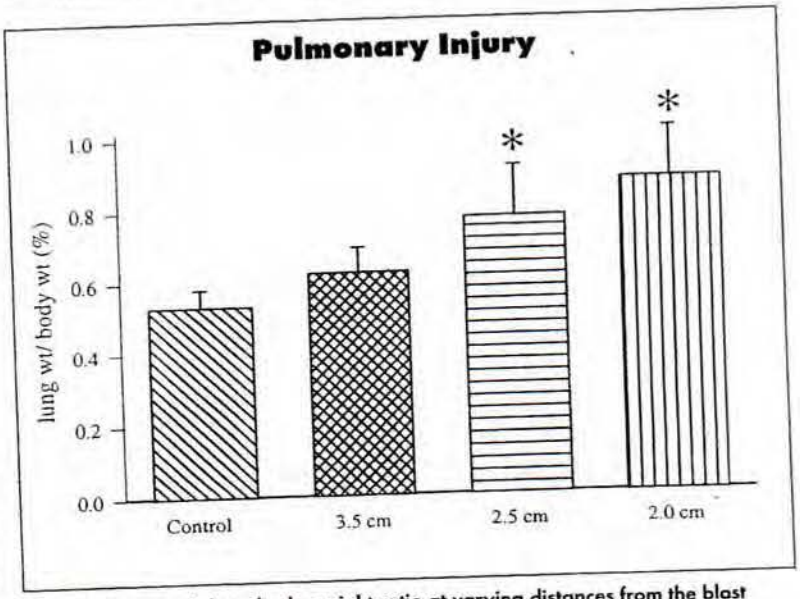

Figure 6: Lung weight to body weight ratio at varying distances from the blast wave generator. * p≤0.05 vs control.

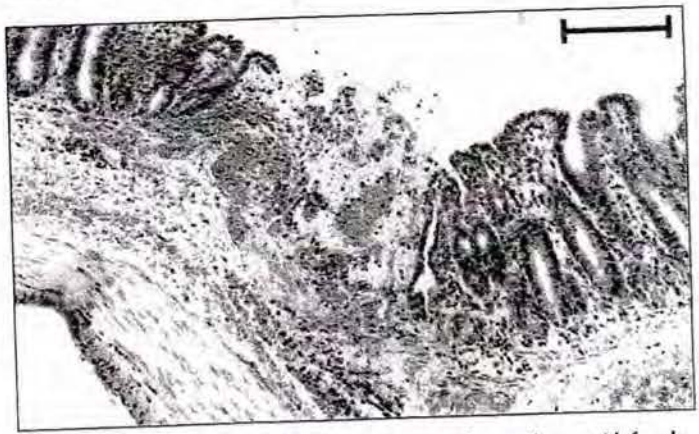

Figure 7: Photomicrograph of subserosal bowel hemorrhage with focal areas of necrotic crypt and villi. Bar = 1.0 mm.

compressive strain and deformation of the chest and abdominal walls[2,12,13] and direct transfer of the blast wave into the body parenchyma leading to injury by spalling, implosion and inertia.[14,15] Lung injury among our rats was most commonly seen in the lower lobes, probably from compression in the costophrenic sinus. The characteristics of "blast lung" occurred regularly in our model with increasing damage seen following higher intensity blasts.

Air emboli is thought to be the predominant cause of immediate death after blast wave injury[10,16] and are difficult to detect because of rapid air absorption in the capillaries. Emboli arise from air injected into a blast-induced alveolar-venous fistula that flows into the systemic circulation and the cerebral and coronary arteries.[10,16,17] Air emboli were seen histologically in the 2.5 and 2.0 cm group and grossly in the systemic arterial circulation of a few animals of the 2.0 cm group.

The intestines, an occasional site of blast wave injury, classically develop subserosal hemorrhage that arises from shear stress between the mucosa and the muscular layers.[14] Damage occurs most commonly in areas with large gas pockets such as the stomach and cecum.[18,19] Focal areas of intestinal necrosis is probably due to ischemia from air emboli and may result in delayed perforation.[19] In our study, subserosal hemorrhage and microscopic evidence of villi and crypt necrosis were identified in a small number of animals.

Blunt trauma resulting in liver fracture and hemoperitoneum were seen more frequently in animals exposed to higher intensity blast, apparently caused by the compressive effects of the blast wave upon the body.

Conclusion:

In this study, we developed a blast wave generator that produces pressure waves similar to high energy explosives and produced pathologic injuries in rodents that appeared identical to clinical case reports and previous animal experiments. This blast wave generator allows an inexpensive, safe method to study global primary blast injury. This method avoids the dangers of open field explosives, the expense of complex shock tubes, and allows the observer immediate contact with the animal in a laboratory setting. This model provides a powerful tool for studying the pathophysiology and potential treatments of bomb blast victims.

Acknowledgements

The authors greatly appreciate the efforts of Joel Young in the design and construction of the blast wave generator and Wayne Templeton for his expertise and technical assistance. We wish to recognize Theresa J. Lander and Son V. Do for analysis of the data and construction of the graphs presented in this study.

References

1. Cook, MA. *The Science of High Explosives*. New York, NY: Reynolds Publishing Corporation, 1958, pp 1-100.
2. Maynard RL, Cooper GJ. Mechanism of Injury in bomb blasts and explosions. In Westaby S (ed): *Trauma - Pathogenesis and Treatment*. London: Heinemann, 1988, pp 30-41.
3. Cooper GS, Maynard RL. Casualties from terrorist bombings. *J Trauma* 1983, 23: 955-967.
4. Desaga H. Blast Injuries. In: *German Aviation Medicine, World War II, Vol. 2*, U.S. Dept. Air Force, 1950, pp 1274-1293.
5. Moolenbeck C, Ruitenberg EJ. The 'Swiss Roll': A simple technique for histologic studies of the rodent intestines. *Laboratory Animals* 1981, 15:57-59.
6. Krohn PL, Whitteridge D. Physiological effects of blast. *Lancet* 1942, 1:252-275.
7. Caseby NG, Porter MF. Blast injuries to the lungs: Clinical presentation, management and course. *Injury* 1977, 8: 1-11.
8. Coppel DL. Blast injuries to the lungs. *Br J Surg* 1976, 63: 735-737.
9. Mellor SG. The pathogenesis of blast injury and its management. *Br J Hosp Med* 1988, 39:536-539.
10. Benzinger T. Physiological effects of blast in air and water. In: *German Aviation Medicine, World War II*, Vol. 2, U.S. Dept. Air Force, 1950, pp 1225-1259.
11. Hooker DR. Physiologic effects of air concussion. *Amer J Physiol* 1924, 67:219.
12. Zuckerman S. Experimental study of blast injuries to the lungs. *Lancet* 1940, 2:219-224.
13. Yen RJ, Fung YC. Trauma of lung due to impact load. *J Biomechanics* 1988, 21:745-753.
14. Schardin H. The physical principles of the effects of a detonation. In: *German Aviation Medicine, World War II*, Vol. 2, U.S. Dept. Air Force, 1950, pp 1207-1224.
15. Clemendson CJ, Frankenberg L. Dynamic response of thorax and abdomen of rabbits to partial and whole-body blast exposure. *Am J Physiol* 1969, 216:615-20.
16. Clemendson CJ, Hultman HJ. Air embolism and the cause of death in blast injury. *Milit Surg* 1954, 114: 424-437.
17. Rössle R. Pathology of blast effects. In: *German Aviation Medicine, World War II*, Vol. 2, U.S. Dept. Air Force, 1950, pp 1260-1273.
18. Harmon JW, Haluszka. Care of blast injured casualties with gastrointestinal injuries. *Milit Med* 1983, 148: 586-588.
19. Cameron GR, Short RH. Physiological changes produced in animals by depth charges. *Br J Surg* 1942, 30:49-64.

The Authors

Randy J. Irwin, MD, is chief resident of general surgery at the University of Oklahoma College of Medicine. Megan R. Lerner is an instructor in the Department of Surgery and is supervisor and coordinator of the surgical research labs at the University of Oklahoma College of Medicine, Health Sciences Center, Oklahoma City. John F. Bealer, MD, is currently a pediatric surgeon in Denver, Colo. He was chief resident in the Section of Pediatric Surgery at the University of Oklahoma College of Medicine, Health Sciences Center, Oklahoma City. Stan A. Lightfoot, MD, is an assistant professor of pathology at University of Oklahoma College of Medicine, Health Sciences Center. Daniel J. Brackett is an associate professor in the Department of Surgery and is director of research, University of Oklahoma College of Medicine, Health Sciences Center. David W. Tuggle, MD, is assistant professor and chief of the Section of Pediatric Surgery at the University of Oklahoma College of Medicine, Health Sciences Center.

Morris water maze: procedures for assessing spatial and related forms of learning and memory

Charles V Vorhees & Michael T Williams

Division of Neurology (MLC 7044), Cincinnati Children's Research Foundation and Department of Pediatrics, University of Cincinnati College of Medicine, 3333 Burnet Ave., Cincinnati, OH 45229-3039, USA. Correspondence should be addressed to C.V.V. (charles.vorhees@cchmc.org)

Published online 27 July 2006; doi:10.1038/nprot.2006.116

The Morris water maze (MWM) is a test of spatial learning for rodents that relies on distal cues to navigate from start locations around the perimeter of an open swimming arena to locate a submerged escape platform. Spatial learning is assessed across repeated trials and reference memory is determined by preference for the platform area when the platform is absent. Reversal and shift trials enhance the detection of spatial impairments. Trial-dependent, latent and discrimination learning can be assessed using modifications of the basic protocol. Search-to-platform area determines the degree of reliance on spatial versus non-spatial strategies. Cued trials determine whether performance factors that are unrelated to place learning are present. Escape from water is relatively immune from activity or body mass differences, making it ideal for many experimental models. The MWM has proven to be a robust and reliable test that is strongly correlated with hippocampal synaptic plasticity and NMDA receptor function. We present protocols for performing variants of the MWM test, from which results can be obtained from individual animals in as few as 6 days.

© 2006 Nature Publishing Group http://www.nature.com/natureprotocols

INTRODUCTION

Many water mazes have been developed, but the one that is referred to as 'the water maze' was developed by Richard Morris[1]. The maze was designed as a method to assess spatial or place learning and herein will be referred to as the Morris water maze (MWM). Morris described the basic procedures in 1984 (ref. 2) and subsequently added details and procedures for assessing related forms of learning and memory[3]. Several characteristics have contributed to the prevalent use of the MWM. These include the lack of required pretraining, its high reliability across a wide range of tank configurations and testing procedures, its cross species utility (rats, mice and humans (in a virtual maze[4])), extensive evidence of its validity as a measure of hippocampally dependent spatial navigation and reference memory[5], its specificity as a measure of place learning, and its relative immunity to motivational differences across a range of experimental treatment effects that are secondary to the central purpose of the task (genetic, pharmacological, nutritional, toxicological and lesion). Although the latter is a general characteristic shared by all water mazes[6], the MWM capitalizes on this strength. For example, hippocampal and septohippocampal lesions in rats reliably induce hyperactivity, but such animals show deficits in the MWM[7]. At the opposite pole, treatments that induce hypoactivity can be dissociated from learning deficits in the MWM. For example, it has been shown that MWM learning impairments are independent of locomotor effects because land based locomotor reductions did not affect swimming speed. Moreover when the experimental animals have deficits during probe trials, this further dissociates learning from performance because measures recorded on probe trials are insensitive to swimming speed[8].

The use of the MWM in assessing learning and memory has been reviewed[9,10], as has the relationship between performance in the MWM and both neurotransmitter systems and drug effects[11]. MWM performance has been linked to long term potentiation (LTP) and NMDA receptor function[12–15], making it a key technique in the investigation of hippocampal circuitry. In addition, it has been shown that there is involvement of the entorhinal and perirhinal cortices, as well as involvement of the prefrontal cortex, the cingulate cortex, the neostriatum, and perhaps even the cerebellum in a more limited way[10].

Despite extensive use of the MWM, the task has not always been used optimally. Some of this stems from an under appreciation for the aspects of the apparatus and testing procedures that are most salient for obtaining the best possible data. Here, we provide a description of the apparatus, its key features, and protocols that are effective and reliable for detecting drug/lesion induced changes in spatial learning and memory[16–20] or changes that arise as a result of genetic manipulations[21–28]. We also provide variations to the basic protocol that can be used to enhance assessment of spatial navigation and/or test for related types of learning (latent, discrimination, and cued learning or working memory).

The MWM is not a maze in the usual sense that is, it is not a labyrinth; rather, it is an open circular pool that is filled approximately half way with water. The interior is made such that it is as close to being featureless as possible. It is a 'maze' in the sense that the animal must search in order to locate a relatively small goal (a hidden platform) that is submerged below the water surface and placed in a fixed location. The platform is camouflaged either by placing opacifying materials in the water (typically, tempera paint or polypropylene pellets), by creating a nearly invisible platform to background color match, or by using transparent platforms against a colored background, thereby making it indistinct given the low visual aspect ratio to the water as seen by the animal when swimming.

It is standard to designate two principal axes of the maze, each line bisecting the maze perpendicular to one another to create an imaginary '+'. The end of each line demarcates four cardinal points: North (N), South (S), East (E) and West (W). These are not true magnetic compass directions but refer to S being the experimenter's position, N being at the opposite point, E being to the experimenter's right and W being to the experimenter's left. Dividing the maze this way creates four equal quadrants. The platform is

positioned in the middle of one of the quadrants. One can either keep the platform in one quadrant for all trials or test one quarter of the animals with the platform in each of the quadrants. The latter approach counterbalances for possible quadrant effects. One can even use eight different platform positions[22]. The platform is usually located half way between the center and the wall, regardless of the quadrant selected, although other arrangements are sometimes used[29].

Test protocols

Spatial acquisition. Place or spatial learning is the most basic MWM procedure. The concept behind it is that the animal must learn to use distal cues to navigate a direct path to the hidden platform when started from different, random locations around the perimeter of the tank. If there are no proximal cues available, the use of distal cues provides the most effective strategy to accomplish this. Most protocols use four start locations: N, S, E and W. Animals are given a series of daily trials using a random or semi random set of start locations. Semi random start position sets are most common, such that the four positions are used, with the restriction that one trial each day is from each of the four positions. A few investigators use eight start locations[30]. One concern about the cardinal start positions is that they are not equidistant from the goal, creating short and long paths to the goal. Even in a large maze, a rat starting at E, with the goal located at SE, has a short path to the goal. There is no perfect solution to this problem. A partial solution that we have used is to use only distal start locations[18]. By this, we mean that if the goal is SE, then one can use start locations of N, W, NE and SW. Although not equidistant from the goal, these start positions are closer to being equal in length than using start positions that are adjacent to the goal. Another approach might be to use only two start positions, such as N and W only, but one must then be concerned that animals might memorize specific routes rather than use distal cues. A third approach is to use three start positions, each in quadrants other than the one containing the platform[31], however only two of these are equal in length.

Table 1 illustrates a set of semi randomly selected distal start positions for basic acquisition training, with the platform being located in the SW quadrant. These are designed so that the animal is not able to learn a specific order of right or left turns to locate the platform, while using each of the four start positions once each day. As can be seen in **Table 1**, the learning trials are conducted over 5 days, with 4 trials per day. The interval between trials can vary from 10 15 s to 5 15 min. If an animal fails to find the platform within the allotted time, it is usually picked up and placed on the platform for ~15 s, although some prefer to guide the animal to the goal based on evidence that it is the middle portion of the swim path that seems to be most important in learning how to navigate to the goal[32].

To assess reference memory at the end of learning, a probe (transfer) trial is given. The most common method is to administer one probe trial 24 h after the last acquisition day. With some procedures, the probe trial is administered immediately following the last learning trial; however, this cannot differentiate between short and long term memory, as it may reflect memory for the most recent training session. A long interval between the last training trial and the probe trial is essential if reference memory is to be determined independent of the memory of the last training session.

TABLE 1 | Morris water maze spatial (hidden platform) start positions.

Acquisition				
Day	**Trial 1**	**Trial 2**	**Trial 3**	**Trial 4**
1	N	E	SE	NW
2	SE	N	NW	E
3	NW	SE	E	N
4	E	NW	N	SE
5	N	SE	E	NW
6 (Probe)	NE			
Reversal				
Day	**Trial 1**	**Trial 2**	**Trial 3**	**Trial 4**
1	S	W	NW	SE
2	NW	S	SE	W
3	SE	NW	W	S
4	W	SE	S	NW
5	S	NW	W	SE
6 (Probe)	SW			

Example of start positions using distal locations for which the goal (platform) is located in the SW quadrant during acquisition and in the NE quadrant during reversal. The sequences of starts are designed such that the goal will be to the right or left of an animal during an equal number of trials and one trial will occur from each of the four start positions each day.

Additional probe trials are sometimes interspersed during the learning phase: these are often given before the first learning trial of the day. These additional probe trials may help to determine the rate of memory consolidation, as this allows the gradual emergence of goal quadrant preference to be seen across days. However, caution should be exercised not to conduct too many probe trials as these are extinction trials and may slow the rate of learning.

Spatial reversal. It is increasingly common and frequently informative to relocate the platform to another quadrant (usually the opposite one) and administer another set of four trials per day for 5 additional days (**Table 1**). This is often called reversal learning, although the term is not precise, as swimming to an opposite quadrant is not the mirror image of the initial problem as it is in a T maze. Reversal learning in the MWM reveals whether or not animals can extinguish their initial learning of the platform's position and acquire a direct path to the new goal position. Tracking patterns typically reveal that mice swim to the previous location first, then begin to search in an arching pattern to reach the new goal (**Fig. 1**). Even after multiple trials, mice do not entirely abandon their initial learning strategy and begin trials by starting to move towards the original platform position, then turn and swim more directly to the new goal. Rats, on the other hand, rapidly switch their search strategies to the new goal position (**Fig. 2**). In fact, rats switch away from the old goal location so rapidly that return visits to the original platform location above chance (i.e., 25%) cannot be seen in the average of the first four trials on reversal day 1 but may be seen on individual trials within the first day of reversal testing. As in the acquisition phase, at the end of the reversal phase, a reversal probe trial is given 24 h later.

Spatial double-reversal with a smaller platform. Many variations can be added to the basic MWM procedures and these can add valuable information for understanding the deficits that are observed or may even unmask more subtle deficits that are not seen during acquisition or reversal learning. One procedure that has

© 2006 Nature Publishing Group http://www.nature.com/natureprotocols

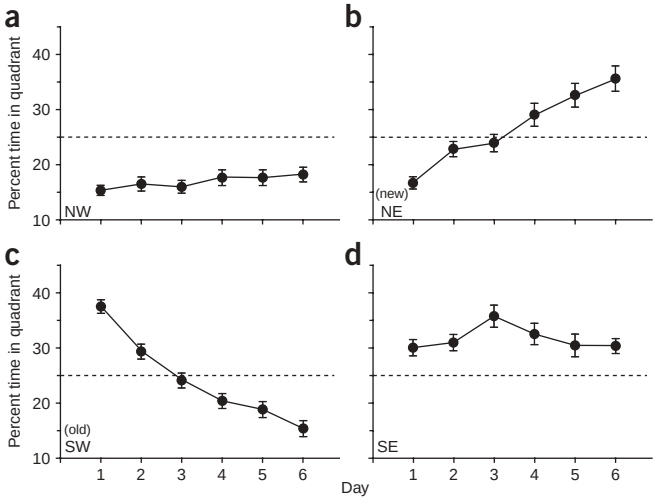

Figure 1 | Percent time in each quadrant of Morris water maze performance on each day of testing in C57BL mice. The results were averaged across four trials per day (mean ± s.e.m.) in untreated C57BL male mice during the reversal phase of learning that is, after 6 days of acquisition training in which the platform was in the SW quadrant. During the trials shown (**a d**), the platform was moved from the SW to the NE quadrant. The gradual reduction in percent time can be seen in the 'old' or previous SW goal quadrant and the gradual shift to the 'new' NW goal position (tank diameter, 122 cm).

been effective in our hands has been to move the platform again, either back to the original goal (double reversal) or to a different quadrant (shift), but with an additional change: use of a smaller platform[17]. For example, if the starting platform is 10 × 10 cm, the reduced platform may be 5 × 5 cm. This reduction in platform size taxes the spatial accuracy requirements of the animal and has revealed the effects of some drugs or doses that are not seen during acquisition or reversal[16,20]. A reduced platform probe trial is also given 24 h after the end of this phase of testing.

Repeated learning. Another procedure is to conduct a set of reversal or shift phases serially[19]. This allows an examination of the animals' flexibility in their ability to learn across multiple phases of new learning. The data also demonstrate the effects of moving the platform to different quadrants. For example, if the platform is shifted to an adjacent quadrant, new learning is more rapid than if shifted to an opposite quadrant[19].

Spatial working memory. The procedures described above are for the assessment of trial independent learning (that is, the goal does not move from trial to trial during a given phase of testing). To assess working or trial dependent learning and memory, a different method is required. In this procedure, which is also called match ing to sample, the platform is relocated every day and the animal is given two trials (or more) per day (see **Table 2**). On each day, the first trial represents a sample trial. During the sample trial, the animal must learn the new location of the platform by trial and error. Trial 2 (or any successive trial) is the test or matching trial in which savings in recall between Trial 1 and Trial 2 are measured. Trial 2 begins after a 15 s inter trial interval. If the animal recalls the sample trial, it will swim a shorter path to the goal on the second trial. As the platform is moved daily, no learning of platform position from the previous day can be transferred to the next day's problem; hence, recall on each day during Trial 2 is dependent on that day's sample trial and measures only temporary or working memory.

Discrimination learning. The MWM can also be used to assess visual discrimination learning[3]. In this procedure, two visible platforms are used that are distinct from one another such as one being white and one being black. One is the standard fixed platform that is raised above the water and the other platform floats from a tether. The task for the subject is to learn which platform can be used for escape from the water and which cannot. The accuracy of the animal's choice across successive trials is an index of its ability to differentiate the stimulus information of the 'true' goal relative to the 'false' goal.

Latent learning. In latent learning, the idea is to place the animal on the platform before each trial rather than after. This will allow one to determine how much of the spatial learning stems from navigating to the platform compared with orientation to the goal once there. Morris has described this procedure elsewhere[3].

Cued learning. A control condition that is frequently used in the MWM is to test the animals for their ability to learn to swim to a cued goal. In this procedure, curtains are closed around the maze to reduce the availability of distal cues. The curtains interfere with the animal's access to distal cues that could be used to spatially navigate. The platform is the same as in the hidden platform version, except that it is either elevated above the water surface[19] or is kept submerged but a 'flag' is mounted that extends above the water surface by approximately 12 cm (ref. 33). Although both methods work, we find that the version with a flag seems to be more efficient, as it is readily recognizable from across the pool, whereas

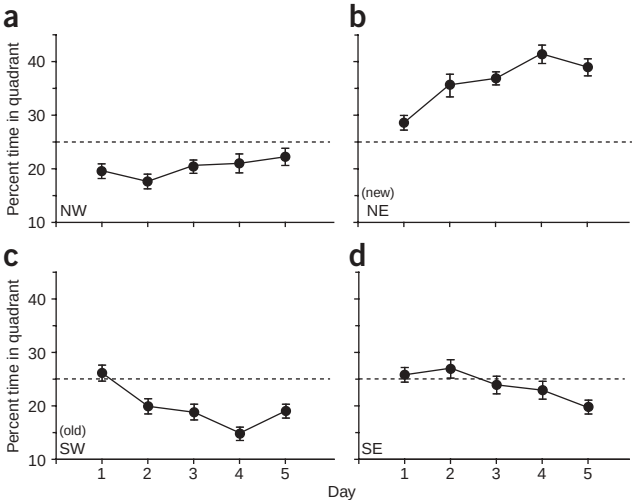

Figure 2 | Percent time in each quadrant of Morris water maze performance on each day of testing in Sprague Dawley rats. The results were averaged across four trials per day (mean ± SEM) in untreated Sprague Dawley male rats during the reversal phase of learning, as in **Figure 1**. The platform was in the SW quadrant during acquisition training and, during the trials shown (**a d**), the platform was moved from the SW to the NE quadrant. As can be seen, rats show a rapid switch from the 'old' SW position to the 'new' NE platform position without perseverating on the original platform quadrant (tank diameter, 210 cm).

© 2006 Nature Publishing Group http://www.nature.com/natureprotocols

TABLE 2 | Sequence of start and goal positions for assessing trial-dependent (working) spatial learning and memory.

Day of acquisition	Start	Goal
1	N	SE
2	E	NE
3	S	SW
4	W	SE
5	S	NE
6	N	NW
7	W	NE
8	E	SE
9	W	NW
10	S	SE
11	E	SW
12	N	SW
13	E	NW
14	W	NE
15	N	SE
16	S	SW
17	N	NE
18	S	NW
19	E	NW
20	W	SW
21	N	SE

Two trials are given per day and both trials use the identical start and goal locations as listed.

the protruding platform may not be. This 'cue' is designed to allow the animal a direct line of sight to the platform's location. To ensure that the animal is using this proximal cue to locate the platform, the location of the goal and the start are both moved to new positions during each trial (**Table 3**). In this way, the subject cannot use distal cues to solve the problem. The only cue that reliably indicates the location of the platform relative to the start is the cue that is attached to the platform. Morris introduced this as a control procedure as part of his original description of the test[1]. Unfortunately, this procedure is all too often omitted, yet its value is unmistakable. If subjects are impaired in cued learning, there is a potentially serious concern about whether a spatial deficit is present. This is because cued learning requires the same basic abilities (intact eyesight, motoric ability (swimming), basic strategies (learning to swim away from the wall, learning to climb on the platform)) and the same motivation (escape from water) as the spatial version of the task. Therefore, if the subject cannot perform the cued task, doubt is cast on its capacity to learn using distal cues in the spatial version. This task can be administered before or after the spatial version, but administering it before has advantages, especially for mice. Some animals find the platform, but then jump back into the water and continue searching. Presumably, this reflects an effort to find another route of escape. In the first few trials, some animals are sufficiently activated by being in the water that it is not always clear that they recognize that the platform is an escape when they first locate it. Therefore, testing animals first in cued trials eliminates the problem of animals not acquiring the appropriate subordinate skills before they are presented with the spatial version of the task.

TABLE 3 | A cued learning trial pattern.

Test day	Trial 1	Trial 2	Trial 3	Trial 4
1	N–SE	E–NE	S–SW	W–SE
2	S–NE	N–NW	W–NE	E–SE
3	W–NW	S–SE	E–SW	N–SW
4	E–NE	W–NE	N–SW	S–SW
5	N–NE	S–NW	E–NW	W–SW
6	S–NE	W–SW	E–SW	N–NE

The first letter denotes the start position and the second letter denotes the goal position.

Control procedures

Cued learning is basically a control procedure, but it is not the only one available. For example, Cain[34–36] has shown that some drugs interfere with sensorimotor function and this can interfere with the animal's ability to recognize that the platform is the goal. He has proposed several ways of determining whether sensorimotor interference is occurring. He suggests measuring thigmotaxis, or the tendency to cling or follow the wall around the outer perimeter of the tank, as one index to reflect that the animal is not problem solving. Excessive thigmotaxis (especially in rats) indicates that the animal is not focusing on the task appropriately because one of the first things that animals have to learn is that there is no escape located around the perimeter of the tank. Having learned this, most animals swim away from the wall and then, by weaving or looping search patterns, eventually find the platform. Not learning this basic approach indicates that the animal may not have adequate awareness of its surroundings. Other measures of impaired sensorimotor interference are excessive jump offs, swimovers and/or deflections. Rats that reach the platform but do not climb on it, or do not stay on it, are not acquiring the requisite association between the platform and escape. Some of these behaviors may be seen during early trials even in control animals, but these usually disappear within a day. If such behaviors are more frequent in the experimental group, however, questions should be raised about whether spatial learning can be satisfactorily assessed.

Cain has suggested that one way to solve the problem of sensorimotor interference is to compare two groups of experimental animals: one tested in the standard procedure and one pretrained using a 'non spatial' training procedure. The pretrained group is given a series of hidden platform trials in which the start and goal are moved randomly on every trial, as is done in cued learning, but here the curtains are left open and the platform is hidden. The task cannot be solved using spatial navigation because of the randomized start goal combinations but it teaches the subject the basic task requirements — namely, the escape can only be found by searching, the goal is located somewhere away from the wall and the platform is the goal. Cain[34–39], Morris[15] and Whishaw[40] have demonstrated that 'non spatial' pretraining can separate components of learning that are not spatial from those that are and this, in turn, can change the interpretation of the findings. As non spatial or strategy pretraining and cued training both have the effect of teaching animals the basic task requirements and tend to eliminate behaviors such as swimovers, jump offs and even diving, it can be helpful to conduct cued trials first. Strategy pre training is not usually necessary unless the data show that thigmotaxis or platform recognition behaviors indicate that sensorimotor problems are present. Acute pharmacological studies, however, may need non spatial pretraining to ensure that non cognitive effects are not interfering with maze performance, whereas delayed or long term drug effect studies may not need this extra procedure.

© 2006 Nature Publishing Group http://www.nature.com/natureprotocols

Another approach to determine whether or not animals have any underlying sensorimotor deficits is to assess swimming speed. Often this is done in the maze during learning trials[41]. Alternatively, one can pre test animals in a separate apparatus, such as a long, straight swimming channel. We use a 15 × 244 cm water filled channel with an escape ladder or platform at one end[33], although shorter channels have also been used[31]. This task requires virtually no searching, hence virtually no learning. The first one or two trials serve to acclimate them to swimming and the rats quickly recognize that the escape can be found by simply swimming from one end to the other. During subsequent trials (a total of four is typical), rats swim as fast as they can to get from the start to the goal. This provides a measure of basic swimming ability and motivation to escape from water, and can be used to determine whether or not animals are motorically and motivationally equivalent across groups prior to MWM trials. An analysis of the average of these trials or use of the fastest trial provides assurance that MWM trials can be interpreted correctly.

Summary of the MWM

Spatial mapping versus working memory hypotheses and the data supporting each using the MWM has been reviewed in detail elsewhere[5,42]. There are many tests that have been used to assess these functions, of which the MWM is but one. However, the MWM has become an important, even dominant, method. As with all methods, the MWM has strengths and weaknesses; however, most of its perceived weaknesses arise from the use of mazes that are too small, protocols that do not adequately assess learning, failure to provide an appropriate interval between training and probe trials to assess reference memory, or lack control procedures to assess non spatial factors. Despite this, the MWM has become more widely used than its predecessors (radial arm maze, passive avoidance, T mazes and their variations) since its introduction 25 years ago. This increased utilization arises because the effects on MWM performance after treatment have been more widely repli cated than the effects observed with any other learning task, and the MWM is relatively straightforward to set up. There can be little doubt that the MWM has significantly advanced our understand ing of the relationship between NMDA receptors, synaptic plasti city and learning[43], and it continues to be used in new applications for the assessment of other types of learning. As use of the task has grown, so too have the number of methodological variations, some of which have extended its utility. The protocols described here provide guidance that can help users avoid the most common pitfalls.

The MWM is primarily a test of spatial learning and reference memory and that remains its principal strength. Detailed analyses have shown that rats can solve the task using a minimal set of cues that involve angular separation and distance from the tank wall[29]. Such data show that when properly configured and utilized, with the inclusion of appropriate control procedures, the MWM is a powerful technique for assessing spatial mapping. Appropriate modification of the basic protocol makes it a flexible tool that can be applied to probe spatial learning in more depth or to assess other forms of learning and memory.

MATERIALS

ANIMALS

- Rats: Albino strains (such as Sprague Dawley, Wistar, Fischer 344 and Lewis) learn well, despite reduced eye pigmentation, as do pigmented strains (such as Long Evans and Listar).
- Mice: Many labs report that C57BL mice are among the best performers in the MWM test[44,45]; however, many other strains and hybrids have been used (see GENETIC BACKGROUND).

Either rats or mice may be used, as described above.

! CAUTION Experimenters must comply with national regulations concerning animals and their use.

EQUIPMENT SETUP

The Maze Morris' original maze was 130 cm in diameter[1] but he later introduced a larger 214 cm diameter maze[2]. Thereafter, he refers to a maze of 200 cm diameter[5] (see also ref. 46). Here, we will describe two apparatuses: one for rats and one for mice. Both are stainless steel circular tanks. The one for rats is 210 cm in diameter and the one for mice is 122 cm in diameter. Both have sides that are 51 cm in height with non reflective interior surfaces. For albino rats, the inside of the larger maze is painted black, whereas for C57BL mice, the inside of the smaller maze is painted white. Because the area of the surface increases with the square of the radius, larger tanks present a much more difficult spatial problem because of the greatly expanded search area to target ratio. The maze is typically mounted above the floor and plumbed with a drain line and valve to facilitate cleaning.

! CAUTION Commercially available swimming pools and troughs are often used as MWM tanks, but caution should be exercised with these as they often have prominent welded seams, corrugated surfaces or other features that pro vide proximal cues that is, markings inside the tank. Such cues undermine the goal of the task, as the purpose is to test the animal's ability to navigate using distal cues. Having a tank that is professionally constructed with atten tion to unobtrusive seams and a uniform interior is worth the investment. Smooth interior walls also minimize the attempts of animals to climb the walls during early trials.

The platform The goal (platform or target) can be either square or circular and is usually 10 or 11 cm^2 or 10 12 cm in diameter, and is typically submerged 1 2 cm below the surface, although with mice this depth is often reduced to 0.5 1 cm. We find it instructive to use smaller platform sizes for some phases of learning to increase task difficulty. Task difficulty is a function of the ratio of search area to target size. For example, a 210 cm diameter tank and a 10 cm^2 platform, as we use, has a search area:target ratio of 346:1, whereas a 122 cm diameter tank and a 10 cm^2 platform has a ratio of 117:1. These ratios work well for rats and mice, respectively. A reduction of the platform size to 5 cm^2 increases this ratio to 1385:1 in the large tank and 468:1 in the small tank. We have previously compared the latencies for animals tested using a ratio of 346:1 (10 cm^2 platform) or 1385:1 (5 cm^2 platform) from the beginning of acquisition. We found that, although animals that are trained with the 10 cm^2 platform learned the task to asymptotic performance within ~20 trials, it took much longer using the 5 cm^2 platform and performance never reached the same level as it did in the 10 cm^2 platform trained group[47]. Therefore, starting out with a small platform makes the task too difficult. Smaller platforms are best reserved for later phases of testing, after the animal has learned the basic task with a larger platform. Research on the effect of tank diameter to target size is limited, but this ratio clearly is an important variable[48].

Platforms are typically made of acrylic or PVC. There are several types, the most common being the use of an acrylic dowel or PVC pipe as the vertical post, with the platform mounted on the top (often with small holes or some other textured surface to provide traction). The base is usually a larger piece of acrylic that rests on the bottom of the pool and is large enough to provide stabi lity so that it will not tip when the animal climbs on it and it resists movement when an animal bumps it. Another approach is to use a submerged acrylic disk with holes in it that the platform dowel fits in. This prevents erroneous position ing of the platform and makes it easier to precisely relocate the platform to other positions during different phases of testing. There are also platforms that can be raised and lowered (e.g., Atlantis On Demand platforms, or by other means[31]). Most acrylic plastics have specific gravities <1.0, so these materials often require that weight be added. Selection of high density acrylic avoids this problem.

Water A common concern is water temperature. It was originally suggested that rats need water to be warmer than typical ambient air

© 2006 Nature Publishing Group http://www.nature.com/natureprotocols

temperatures that are found in most laboratories (19 22 °C), but this has not been widely borne out. Rats tested in water that has been equilibrated to ambient temperatures of 19 22 °C perform well and do not show evidence of significant fatigue or hypothermia at typical test ages[49]. However, the situation in mice may be different (see below).

Room configuration The maze should be placed in a room with ample surrounding visual cues. These distal cues can be intentional or can be endogenous to the room; however, it is critical that the cues are not moved during testing as these are the animal's navigational reference points for locating the goal, independent of start location. The distance of cues from the outside wall of the maze can also be important (see ref. 29). Because some labs are relatively barren, when in doubt it is prudent to add cues; there is no evidence that too many cues are a problem, but too few may be. It is useful to mount curtains around the maze. These may be used to position intentional cues should testing of the effects of cue rotation be desired, but the principal reason to have curtains is to obscure distal cues during cued learning trials (see above).

Experimenter Experimenter effects in the MWM principally involve animal handling and effects of experimenter visibility. Handling issues are the same as for any experiment that assesses behavior and will not be discussed here.

The position of the experimenter can be handled in several ways: the experimenter can: (a) leave the room during testing; (b) stand behind a visual barrier; or (c) remain stationary in a constant location. The latter is the most common but it should not be forgotten that the experimenter then becomes one of the distal cues. Animals that are tested in different quadrants, especially in the distal versus the proximal half of the maze, sometimes show different latencies, depending on whether they are swimming towards or away from the experimenter[50]. This effect does not invalidate the test, but there should be awareness of it and outcomes should not be confounded by allowing an experimenter to move around as they wait for the animal to perform the task.

Lighting Room lighting should be indirect, especially if a video camera, computer and tracking software are used to record performance. Tracking software is sensitive to light reflections from the water surface and these are minimized by indirect lighting.

Tracking system There are many commercial vendors that provide tracking systems that can be used for the MWM. A non exhaustive list includes HVS Image, San Diego Instruments, Accuscan, View Point, Clever Systems, Noldus, Columbus Instruments, Watermaze Software, Coulbourn Instruments, and others. As with any software system, it should be tested on site before selection.

PROCEDURE

Spatial acquisition

1| Place the animal in the desired start position in the maze, facing the tank wall. The animal is released into the water at water-level (not dropped). A timer or computer tracking program is started the moment that the animal is released.

2| Stop the timer when the animal reaches (touches) the platform (most animals immediately climb on the platform but there are exceptions[36]). A trial limit of 1 or 2 min per trial is standard; commonly, 2 min for rats and 1 min for mice. Animals not finding the platform within this time limit are either placed on the platform or guided to it.

3| Leave the animal on the platform during the inter-trial interval (ITI). Inter-trial intervals of 30 or 60 s were once used, but 15 s has become commonplace and produces good learning. However, longer ITIs are often used for mice, especially during the first test session and this improves learning[25]. This may be because mice are more prone to hypothermia-induced performance effects[51]. The objective in leaving the animal on the platform is to allow it to orient to its position in space and remember the position of the goal in relation to surrounding cues. However, this may not be necessary as animals may learn what they need during their navigation to the platform[52]. The latter investigators showed that rats learn the task just as well if the lights are on or off during the ITI when they remain on the platform.

4| Place the animal in the maze at a new start location and repeat the trial (Steps 1–3) until the animal has had the desired number of trials for that day. Animals are normally given multiple trials per day. The most common number is 4. As there are four principal start locations, this keeps the start positions balanced each day. With four trials per day, it takes 5–10 min per animal on the first day and progressively less time per animal each day thereafter. Other trial numbers that have been used are 1 (ref. 23), 2 (ref. 53), 3 (ref. 54), 5 (ref. 55), 6 (refs. 27,56,57), 8 (refs. 52,58), 10 (ref. 59) and 12 (refs. 60,61) trials per day. No large advantage of any one of these trial numbers has been convincingly demonstrated in rats. An alternative approach is to allow the animal 15 s on the platform, then remove it to its cage and test the second animal on Trial 1 and repeat this rotation until all animals have completed Trial 1, then repeat the process for subsequent trials. The latter method improves learning performance in mice[51], but no comparable data exist for rats. There is little evidence to suggest large sensitivity differences as a function of daily trial number, but what evidence there is indicates that having fewer trials per day improves learning[50]. However, this issue has not been sufficiently explored to make definitive recommendations, and tests of trial number have often involved smaller tanks that may not generalize to larger mazes.

5| On subsequent days, repeat the trials. The number of days over which to repeat testing depends on the learning curve. With four trials per day, 5–6 days (20–24 trials) is typically sufficient in a 210 cm maze for rats or in a 122 cm maze for mice to reach asymptotic performance; however, as noted previously, if the task is made more difficult, then more days of testing may be required for animals to reach asymptotic performance. By contrast, rats in a 122 cm maze may approach asymptotic performance by day 2 or 3 (ref. 41).

Reference memory: probe trial

6| Remove the platform.

© 2006 Nature Publishing Group http://www.nature.com/natureprotocols

7| Place the animal in a novel start position in the maze, facing the tank wall — for example, 180° from the original platform position. We use a novel start position during the probe trial to ensure that its spatial preference is a reflection of the memory of the goal location rather than for a specific swim path (see **Table 1**).

8| Remove the animal after a fixed interval (usually 30 or 60 s). There is evidence that quadrant preference decreases after the first 30 s (ref. 41), hence 30 s is recommended. The object of the probe trial is to determine whether or not the animal remembers where the platform was located. Indications of such memory include number of platform-site crossovers, time and distance spent in the target quadrant compared with the other quadrants, time in a pre-defined annulus surrounding the target that is larger than the target itself, average distance to the target site, angle (bearing) to the target site, latency to first target-site crossover, and mean search difference and mean zone difference scores (see ref. 62 for a description of the latter measures). Percent time or percent distance in the target quadrant is used most frequently.

▲ **CRITICAL STEP** Probe trials that are intended to assess reference memory should not be administered shortly after the last learning trial, as this measures recent rather than long-term recall. If an immediate probe trial is given, it should not be a substitute for one given at least 24 h later.

Spatial reversal

9| If spatial reversal tests are desired, relocate the platform to another quadrant (usually the opposite one) and administer another set of four trials per day for 5 days (as described in Steps 1–4).

10| At the end of the reversal phase, perform a reversal probe trial, as described in Steps 6–8.

● TIMING

Each trial is limited to 2 min in rats and 1 min in mice, with an ITI of 15 s and four trials per day. Therefore, it takes no longer than 9 min to complete a learning session. As animals learn, the time per day steadily decreases. Probe trials on the last day are only 30 s. For any phase of testing, 6 days is common: 5 learning days and 1 probe day. The first phase is often cued, followed by acquisition, then reversal, double-reversal, working memory (matching to sample), or other procedures.

? TROUBLESHOOTING

The most common problem is using an improper tank to platform size combination. Many tanks are too small or are at the lower boundary of what constitutes an optimal task for assessing spatial learning. Smaller tanks allow the animal to use other strategies (such as swimming a fixed distance from the wall) to solve the task, while making minimal use of distal cues. Unfortunately, if the tank is too small, animals will learn and the experimenter will not be aware that the animal is using non-distal cues to find the platform and nothing will appear amiss. For this reason, selection of the proper tank size from the outset is the best method for obtaining valid spatial learning.

Using untreated, adult, male, Long–Evans rats, the effect of tank size on performance can be seen in **Figure 3**. The small tank is 122 cm in diameter and the large tank is 210 cm in diameter. Water temperature was the same for both groups, as was platform size (10 cm^2). Both groups received the same number of trials (four per day), in the same order and to the same goal position, on the same days in the same room. The tanks were identically constructed and painted, and the only difference was diameter. For the small tank trials, the smaller perimeter was placed inside the larger one. As can be seen, the small tank group learned the task well; in fact, they learned it so rapidly that there is almost no learning curve. Basically, the small tank group approached asymptotic performance on the second day. By contrast, the large tank group showed a steady improvement in learning up to day 4 and reached asymptotic performance on day 5. It is apparent which curve is better for assessing learning; hence, a 122 cm tank is not recommended for rats.

On the other hand, a 122 cm tank is the most common size that is used for mice. Transgenic, knock-out and knock-in mice are routinely assessed in the MWM for spatial learning. There are ample data that, in mice, good learning curves can be obtained using a 122 cm diameter tank. This may be because this size tank is scaled more to the body size of a mouse or because mice find spatial tasks more difficult than rats and, therefore, a smaller search area is beneficial.

Different mouse strains vary widely in performance during the MWM test. One strain that performs reasonably well is C57BL (ref. 57). Regardless of vendor, C57BL mice are fairly good swimmers and respond to being placed in water with an appropriate swim-search response. Some strains float or turn in circles and cannot be used.

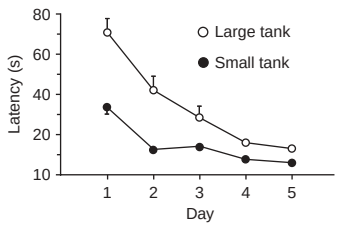

Figure 3 | Morris water maze acquisition performance in untreated adult Long Evans rats. Rats were given four trials per day and data represent the mean ± s.e.m. of blocks of four trials. Data are latency (s) to reach the goal, using identical sequences of start locations. The small tank was 122 cm in diameter and the large tank was 210 cm in diameter. All testing conditions and trials were identical for the two groups. The small tank perimeter was placed inside the larger tank so that all cues were identical. *n* 10 per group (males).

© 2006 Nature Publishing Group http://www.nature.com/natureprotocols

Genetic background

In rats, Sprague–Dawley, Wistar, Long–Evans, Fischer 344, ACI, Dark Agouti and Lewis have all been shown to learn when tested in the MWM.

In mice, the results are consistent that C57BL learn in the MWM, but labs have differed in what they report for other strains. For example, 129S strains in which gene targeting is often performed, have an increased incidence of floating and erratic performance but this may be a function of substrain, as 129S2/SvlmJ mice are reported to perform satisfactorily in the MWM[45]. BALB mice are reported to perform well by some[45] in the MWM and poorly by others[44].

A factor analysis that was designed to locate clustered determinants of MWM learning across multiple mouse strains and a large number of mice ($\sim$1,500) has shown that three factors account for most of the variance in MWM performance[63,64]. The largest factor in mice (48%) was termed thigmotaxis and represents the tendency to swim or float near the tank wall; the second largest factor was termed passivity (20%) and represents slow or non-swimming; and the third factor was memory or goal-directed behavior (13%). The outcome of such an analysis is a function of the factors measured, so different measurements would generate a different factor analysis. Nevertheless, this analysis, which included many important variables of MWM performance, shows that much of the variance in performance is due to factors that are unrelated to learning and memory in mice, hence use of appropriate controls is especially important in mouse studies to arrive at a correct interpretation of results.

Non-performers

Non-performers are rarely encountered in rats, but are seen in mice. Among C57BL mice, non-performers in the MWM are less common than in most other strains. However, some genetic modifications can cause mutant animals to not perform the task. These cases are relatively obvious. However, having a subset of mice that do not search for the goal, because of mixed genetic background or the genetic manipulation under investigation, occurs with some frequency. In such situations, the problem becomes how to handle such cases. The most common problem is that some of the mice float and appear unmotivated to escape. Different methods have been tried to induce non-performers to swim, but these approaches often involve experimenter interventions, such as startling the mouse with a loud noise, prodding it with an object or pre-wetting the fur to reduce buoyancy. Mice are buoyant because their fur coat contains water-repellant oils that allow them to remain floating for minutes at a time. Testing mice in 20–22 °C water generally reduces the frequency of floating. Nonetheless, caution should be used in allowing experimenter interventions. The problem is that interventions are difficult to apply uniformly and may inadvertently introduce bias. If the experimental group has a higher or lower floating frequency or the treatment interacts with startle or other factors, the results could be confounded. A better approach is use of a standard rule that does not involve intervention. Our approach is that if a mouse floats, it is allowed to remain in the water up to the limit of the trial. If the animal fails to swim, it is removed and the next animal is tested. When the other animals in the session are finished, the floater is given a second trial. If it swims, it receives its full trial sequence, with the first trial being excluded from the data. If it floats for the second trial, it is returned to its cage and tested again the next day. If it now swims, it proceeds though the test, staggered one day behind its cohort. If it fails to swim, it is taken out of the test order, as on day 1, until the other animals in the session are tested and is then given one final trial. If it fails to swim during this fourth attempt, it is removed from the experiment. At the conclusion of the experiment, the frequency of floaters in each group is statistically compared to determine whether or not the experimental manipulation significantly altered the frequency of non-performers compared with the wild type. If it does, then the MWM data on those that did swim must be interpreted with caution in light of the possibility of selection bias.

ANTICIPATED RESULTS

Learning trials

Dependent measures of performance on learning trials in the MWM begin with latency (time from start to goal). Latency can be obtained with or without tracking software. Path length is also widely used and has the advantage of being immune to swimming speed. Although path-length determinations have been carried out without the use of a tracking program, these methods are labor-intensive and such data are more easily captured with a tracking program. Another useful index is cumulative distance from the platform; most tracking programs generate this measure as the distance from the platform measured every second or every few milliseconds. Cumulative distance has been suggested to be one of the better measures of spatial learning ability[54]. First bearing and/or mean directionality, which are similar but not identical, measure the animal's swim angle at the start of the trial relative to a direct line from the start to the goal. Angle measurements appear to be sensitive to many types of experimental treatments. In our experience, latency, path length and cumulative distance are highly correlated, whereas first bearing has a lower correlation with these first three measures (**Table 4**). This is logical as the first three measures all reflect aspects of performance across the length of the trial, whereas first bearing is a snapshot of the animal's performance at one particular point during the trial (at the beginning). Other measures are time or distance in the target annulus (the space between two concentric circles, defined by lines touching the outside and inside edges of the platform, respectively — not to be confused with Morris' use of the term 'annulus crossing', by which he means crossings of a zone surrounding where the

© 2006 Nature Publishing Group http://www.nature.com/natureprotocols

TABLE 4 | Correlation coefficient matrix for the four computer-tracked indices of acquisition performance in the Morris water maze.

Variable	Latency	Path length	Cumulative distance	First bearing
Latency	1.00	0.951	0.930	0.409
Path length		1.00	0.971	0.418
Cumulative distance			1.00	0.568
First bearing				1.00

The results were from an experiment in rats having four treatment groups, one of which was significantly impaired in learning and memory during Morris maze testing (from data published in ref. 33).
The percentage of variance that was accounted for by one variable by the other would be the square of each *r*-value (R^2); hence, the variance accounted for is high between variables such as path length and cumulative distance (R^2 0.943), but low between the other variables such as first bearing (e.g., between cumulative distance and first bearing, R^2 0.323).

platform had been) compared with inner or outer annuli (the latter being a measure of thigmotaxis), number of direct swims (number of paths within a preset corridor from the start to the goal) or circle swims (a swim trajectory that approximates a decreasing radius arc of a circle from the start point to the hidden platform and circling is less than 360°), jump-offs, deflections, swimovers, and others. These other measures can be important especially when testing animals that have recently been administered a drug that can disrupt sensorimotor function[36,37].

Probe trials

Site crossings as an index of memory has the limitation that it is variable and often has a low frequency of occurrence, especially if the target is reduced in size or the tank diameter is large. Furthermore, depending on the tracking software, crossover undercounting may occur. We find that the average distance to the target site, time or distance in the target quadrant and first bearing provide more robust measures of memory than exact site crossings. Others report success with target annulus crossovers, where the annulus is a circular zone surrounding and larger than the platform itself.

Data analysis

Acquisition trials are generally averaged in blocks of four and plotted as block means (± s.e.m.), or if larger numbers of trials are used then there may be two or more blocks of trials plotted per day. However, the experimenter should also examine the data by trial to ensure that learning is occurring within each daily test session. Unless an unusual pattern is seen, plotting the data in daily four-trial blocks usually accurately represents the learning process. When daily trials are plotted, long latencies are generally seen during Trial 1 and Trial 2 of day 1, with improvement during Trial 3 and Trial 4. The next day, performance will begin with Trial 1 being longer than Trial 4 of the preceding day, and then performance improving to exceed the performance on Trial 4 of day 1. This saw-tooth pattern repeats on each successive day of testing, with an overall shortening or downward stair-step pattern of performance across days. Plotting the data by blocks of trials smoothes the learning curve and this line is the most widely used index of spatial learning, although other indices have been used (for example, ref. 54).

Data summary and analysis

Group means for each dependent variable should be calculated per trial and per block of trials. Trials 1 and 2 of day 1 of testing should be examined to ensure that the groups do not start the test at different performance levels. The data on the first one or two trials should be compared using a test with high detection power, such as a *t*-test or analysis of variance (ANOVA) if there are more than two groups. If the groups differ significantly during early trials, it is a warning that the groups entered the test with preexisting differences that may prevent or compromise the interpretation of the learning curves or retention trials in terms of spatial learning and reference memory. If the groups are comparable, then the data are typically plotted and analyzed in blocks of trials in order to stabilize the means. Data are generally analyzed by ANOVA. The factors are usually genotype or treatment group and test day. Some experiments will include additional factors, such as sex. Group is generally a 'between'-subject factor and day a 'within'-subject factor in the ANOVA model, although in developmental studies using split-litter designs the factors of group, day and sex may all be within/matching factors. Using statistical programs such as SAS, MWM data may be analyzed using Proc GLM (general linear model) or Proc Mixed. GLM split-plot models can accommodate one or more 'between' and one or more 'within' factors; however, one must be cautious when using GLM models for repeated measure ('within') variables. If there are only two levels of the 'within' factors, the GLM ANOVA solution is precise, but in the MWM there are usually more than two days of testing. With more than two levels of the repeated measure factor, the significance of the 'within' and 'between' *x* 'within' factor F-ratios can be distorted. This is because GLM requires that the data meet the assumption of compound symmetry — that is, that the correlations within the variance-covariance matrix of the repeated factor, say day, be exactly the same at all distances between measurements. For example, the correlation between day 1 and day 2 must be the same as the correlation between day 1 and day 3 or between day 2 and day 3. This assumption is almost never met by learning data because variances change as a function of day as learning proceeds. As animals learn the task, their performance become less variable, hence the variances decrease across days and the correlations change. There is no exact test for compound symmetry, but there is a more stringent test for sphericity. If GLM is used, it is advisable that the covariance matrix test for sphericity be used. If the data are significantly non-spherical, there are adjusted F-ratios that can be used to at least partially correct the F-tests so that significance levels are less likely to be overestimated. The two most common methods of adjusting F-ratios are those of Greenhouse–Geisser and Huyhn–Feldt.

© 2006 Nature Publishing Group http://www.nature.com/natureprotocols

Another approach is to use Proc Mixed ANOVA models (SAS). Proc Mixed ANOVA models provide a more precise way of handling the problem of non-symmetry of the covariance matrix, but Proc Mixed is limited in that it cannot handle more than two 'within' dimensions in the model. However, Proc Mixed has some significant advantages that make it worthwhile. Proc Mixed provides a set of different covariance models that can be fitted to the data. These different models can be tested against the data and compared using best-fit statistics provided by Proc Mixed. In our experience, the AR (1) (autoregressive (1)) covariance model often provides the best fit for MWM learning variables, such as latency, path length and cumulative distance. Regardless of which covariance model best fits the data, the best fit model can be chosen and the data can be analyzed to obtain more precise F-tests than with Proc GLM. Probe data often have no repeated measure component and, therefore, do not require Proc Mixed. Proc Mixed also provides a 'slice' ANOVA option, such that if an interaction is obtained between the factors of group and day, the slice ANOVAs will provide tests of the group effect on each day in order to localize which days show group differences. From this, individual group comparisons (*post hoc* tests) can be made between the treatment groups on selected days; significant interactions or group main effects require the typical considerations of controlling for multiple comparisons. In SAS, Proc Multtest provides group comparison tests that provide different levels of protection against type I errors. The step-down Bonferonni is one such test that we commonly use.

ACKNOWLEDGMENTS The authors acknowledge the support of National Institutes of Health grants DA006733, DA021394, DA014269 and ES007051.

COMPETING INTERESTS STATEMENTS The authors declare that they have no competing financial interests.

Published online at http://www.natureprotocols.com
Reprints and permissions information is available online at http://npg.nature.com/reprintsandpermissions

1. Morris, R.G.M. Spatial localization does not require the presence of local cues. *Learn. Motiv.* **12**, 239 260 (1981).
2. Morris, R. Developments of a water maze procedure for studying spatial learning in the rat. *J. Neurosci. Methods* **11**, 47 60 (1984).
3. Stewart, C.A. & Morris, R.G.M. The watermaze. in *Behavioural Neuroscience, Volume I, A Practical Approach* (ed. Sahgal, A.) 107 122 (IRL Press at Oxford University Press, Oxford, 1993).
4. Kallai, J., Makany, T., Karadi, K. & Jacobs, W.J. Spatial orientation strategies in Morris type virtual water task for humans. *Behav. Brain Res.* **159**, 187 196 (2005).
5. Morris, R.G.M. An attempt to dissociate 'spatial mapping' and 'working memory' theories of hippocampal function. in *Neurobiology of the Hippocampus* (ed. Seifert, W.) 405 432 (Academic Press, New York, 1993).
6. Cravens, R.W. Effects of maternal undernutrition on offspring behavior: Incentive value of a food reward and ability to escape from water. *Dev. Psychobiol.* **7**, 61 69 (1974).
7. Morris, R.G., Garrud, P., Rawlins, J.N. & O'Keefe, J. Place navigation impaired in rats with hippocampal lesions. *Nature* **297**, 681 683 (1982).
8. Fitzgerald, L.W. & Dokla, C.P. Morris water task impairment and hypoactivity following cysteamine induced reductions of somatostatin like immunoreactivity. *Brain Res.* **505**, 246 250 (1989).
9. Brandeis, R., Brandys, Y. & Yehuda, S. The use of the Morris water maze in the study of memory and learning. *Int. J. Neurosci.* **48**, 29 69 (1989).
10. D'Hooge, R. & De Deyn, P.P. Applications of the Morris water maze in the study of learning and memory. *Brain Res. Rev.* **36**, 60 90 (2001).
11. McNamara, R.K. & Skelton, R.W. The neuropharmacological and neurochemical basis of place learning in the Morris water maze. *Brain Res. Rev.* **18**, 33 49 (1993).
12. Jeffery, K.J. & Morris, R.G.M. Cumulative long term potentiation in the rat dentate gyrus correlates with, but does not modify, performance in the water maze. *Hippocampus* **3**, 133 140 (1993).
13. Moser, E.I., Krobert, K.A., Moser, M. B. & Morris, R.G.M. Impaired spatial learning after saturation of long term potentiation. *Science* **281**, 2038 2042 (1998).
14. Morris, R.G.M., Anderson, E., Lynch, G.S. & Baudry, M. Selective impairment of learning and blockade of long term potentiation by an N methyl D aspartate antagonist, AP5. *Nature* **329**, 774 776 (1986).
15. Bannerman, D.M., Good, M.A., Butcher, S.P., Ramsay, M. & Morris, R.G.M. Distinct components of spatial learning revealed by prior training and NMDA receptor blockade. *Nature* **378**, 182 186 (1995).
16. Vorhees, C.V. *et al.* Adult learning deficits after neonatal exposure to D methamphetamine: Selective effects on spatial navigation and memory. *J. Neurosci.* **20**, 4732 4739 (2000).
17. Broening, H.W., Morford, L.L., Inman Wood, S.L., Fukumura, M. & Vorhees, C.V. 3,4 methylenedioxymethamphetamine (ecstasy) induced learning and memory impairments depend on the age of exposure during early development. *J. Neurosci.* **21**, 3228 3235 (2001).
18. Vorhees, C.V., Reed, T.M., Skelton, M.R. & Williams, M.T. Exposure to 3,4 methylenedioxymethamphetamine (MDMA) on postnatal days 11 20 induces reference but not working memory deficits in the Morris water maze in rats: implications of prior learning. *Int. J. Dev. Neurosci.* **22**, 247 259 (2004).
19. Williams, M.T. *et al.* Developmental d methamphetamine treatment selectively induces spatial navigation impairments in reference memory in the Morris water maze while sparing working memory. *Synapse* **48**, 138 148 (2003).
20. Morford, L.L., Inman Wood, S.L., Gudelsky, G.A., Williams, M.T. & Vorhees, C.V. Impaired spatial and sequential learning in rats treated neonatally with d fenfluramine. *Eur. J. Neurosci.* **16**, 491 500 (2002).
21. Ehrman, L.A. *et al.* Phosphodiesterase 1B modulates the effects of methamphetamine on locomotor activity and spatial learning through a DARPP 32 dependent pathway: Evidence from PDE1B DARPP32 double knockout mice. *Genes Brain Behav.* (in the press).
22. Silva, A.J., Paylor, R., Wehner, J.M. & Tonegawa, S. Impaired spatial learning in α calcium calmodulin kinase II mutant mice. *Science* **257**, 206 211 (1992).
23. Bourtchuladze, R. *et al.* Deficient long term memory in mice with a targeted mutation of the cAMP responsive element binding protein. *Cell* **79**, 59 68 (1994).
24. Cho, Y.H., Giese, K.P., Tanila, H., Silva, A.J. & Eichenbaum, H. Abnormal hippocampal spatial representations in αCaMKII^{T286A} and CREB$^{\alpha\Delta}$ mice. *Science* **279**, 867 869 (1998).
25. Upchurch, M. & Wehner, J.M. Effects of N methyl D aspartate antagonism on spatial learning in mice. *Psychopharmacology* **100**, 214 (1990).
26. Grant, S.G.N. *et al.* Impaired long term potentiation, spatial learning, and hippocampal development in *fyn* mutant mice. *Science* **258**, 1903 1910 (1992).
27. Limback Stokin, K., Korzus, E., Nagaoka Yasuda, R. & Mayford, M. Nuclear calcium/calmodulin regulates memory consolidation. *J. Neurosci.* **24**, 10858 10867 (2004).
28. Tang, Y. P. *et al.* Genetic enhancement of learning and memory in mice. *Nature* **401**, 63 69 (1999).
29. Maurer, R. & Derivaz, V. Rats in a transparent morris water maze use elemental and configural geometry of landmarks as well as distance to the pool wall. *Spatial Cogn. Comput.* **2**, 135 156 (2000).
30. Kim, J.J., Lee, H.J., Han, J. S. & Packard, M.G. Amygdala is critical for stress induced modulation of hippocampal long term potentiation and learning. *J. Neurosci.* **21**, 5222 5228 (2001).
31. Markowska, A.L., Long, J.M., Johnson, C.T. & Olton, D.S. Variable interval probe test as a tool for repeated measurements of spatial memory in the water maze. *Behav. Neurosci.* **107**, 627 632 (1993).
32. Sutherland, R.J., Chew, G.L., Baker, J.C. & Linggard, R.C. Some limitations on the use of distal cues in place navigation by rats. *Psychobiology* **15**, 48 57 (1987).
33. Williams, M.T. *et al.* Developmental 3,4 methylenedioxymethamphetamine (MDMA) impairs sequential and spatial but not cued learning independent of growth, litter effects, or injection stress. *Brain Res.* **968**, 89 101 (2003).
34. Saucier, D. & Cain, D.P. Spatial learning without NMDA receptor dependent long term potentiation. *Nature* **378**, 186 189 (1995).
35. Saucier, D., Hargreaves, E.L., Boon, F., Vanderwolf, C.H. & Cain, D.P. Detailed behavioral analysis of water maze acquisition under systemic NMDA or muscarinic antagonism: Nonspatial pretraining eliminates spatial learning deficits. *Behav. Neurosci.* **110**, 103 116 (1996).

© 2006 Nature Publishing Group http://www.nature.com/natureprotocols

36. Cain, D.P., Saucier, D., Hall, J., Hargreaves, E.L. & Boon, F. Detailed behavioral analysis of water maze acquisition under APV or CNQX: Contribution of sensorimotor disturbances to drug induced acquisition deficits. *Behav. Neurosci.* **110**, 86 102 (1996).
37. Cain, D.P. & Saucier, D. The neuroscience of spatial navigation: Focus on behavior yields advances. *Rev. Neurosci.* **7**, 215 231 (1996).
38. Hoh, T.E. & Cain, D.P. Fractionating the nonspatial pretraining effect in the water maze task. *Behav. Neurosci.* **111**, 1285 1291 (1997).
39. Williams, M.T., Vorhees, C.V., Boon, F., Saber, A.J. & Cain, D.P. Methamphetamine exposure from postnatal days 11 to 20 causes impairments in both behavioral strategies and spatial learning in adult rats. *Brain Res.* **958**, 312 321 (2002).
40. Whishaw, I.Q. Posterior neocortical (visual cortex) lesions in the rat impair matching to place navigation in a swimming pool: a reevaluation of cortical contributions to spatial behavior using a new assessment of spatial versus non spatial behavior. *Behav. Brain Res.* **155**, 177 184 (2004).
41. Blokland, A., Geraerts, E. & Been, M. A detailed analysis of rats' spatial memory in a probe trial of a Morris task. *Behav. Brain Res.* **154**, 71 75 (2004).
42. Morris, R.G.M., Hagan, J.J. & Rawlins, J.N.P. Allocentric spatial learning by hippocampectomized rats: A further test of the 'spatial mapping' and 'working memory' theories of hippocampal function. *Quart. J. Exp. Psychol.* **38B**, 365 395 (1986).
43. Morris, R.G.M., Davis, S. & Butcher, S.P. Hippocampal synaptic plasticity and NMDA receptors: A role in information storage? *Phil. Trans. R. Soc. Lond.* **329**, 187 204 (1990).
44. Upchurch, M. & Wehner, J.M. Differences between inbred strains of mice in Morris water maze performance. *Behav. Genet.* **18**, 55 68 (1988).
45. Wahlsten, D., Cooper, S.F. & Crabbe, J.C. Different rankings of inbred mouse strains on the Morris maze and a refined 4 arm water escape task. *Behav. Brain Res.* **165**, 36 51 (2005).
46. Wenk, G.L. *Assessment of spatial memory using the radial arm and Morris water maze.* (eds. Crawley, J.N. *et al.*) Unit 8.5A (Wiley Interscience, New York, 2004).
47. Williams, M.T., Moran, M.S. & Vorhees, C.V. Behavioral and growth effects induced by low dose methamphetamine administration during the neonatal period in rats. *Int. J. Dev. Neurosci.* **22**, 273 283 (2004).
48. Mactutus, C.F. & Booze, R.M. Accuracy of spatial navigation: The role of platform and tank size. *Soc. Neurosci. Abst.* **20**, 1014 (1994).
49. Lindner, M.D. & Ribkoff, V.K. Relationship between performance in the Morris water task, visual acuity, and thermoregulatory function in aged F 344 rats. *Behav. Brain Res.* **45**, 45 55 (1991).
50. Hodges, H. Maze procedures: The radial arm and water maze compared. *Cog. Brain Res.* **3**, 167 181 (1996).
51. Iivonen, H., Nurminen, L., Harri, M., Tanila, H. & Puolivali, J. Hypothermia in mice tested in Morris water maze. *Behav. Brain Res.* **141**, 207 213 (2003).
52. Devan, B.D., Blank, G.S. & Petri, H.L. Place navigation in the Morris water task: Effects of reducted platform interval lighting and pseudorandom plaform positioning. *Psychobiology* **20**, 120 126 (1992).
53. Otnaess, M.K., Brun, V.H., Moser, M. B. & Moser, E.I. Pretraining prevents spatial learning impairment after saturation of hippocampal long term potentiation. *J. Neurosci.* **19** (RC49): 1 5 (1999).
54. Gallagher, M., Burwell, R. & Burchinal, M. Severity of spatial learning impairment in aging: Development of a learning index for performance in the Morris water maze. *Behav. Neurosci.* **107**, 618 626 (1993).
55. Burwell, R.D., Saddoris, M.P., Bucci, D.J. & Wiig, K.A. Corticohippocampal contributions to spatial and contextual learning. *J. Neurosci.* **24**, 3826 3836 (2004).
56. Holscher, C. Stress impairs performance in spatial watermaze learning tasks. *Behav. Brain Res.* **100**, 225 235 (1999).
57. Clapcote, S.J., Lazar, N.L., Bechard, A.R., Wood, G.A. & Roder, J.C. NIH Swiss and Black Swiss mice have retinal degeneration and performance deficits in cognitive tests. *Comp. Med.* **55**, 310 316 (2005).
58. Devan, B.D., McDonald, R.J. & White, N.M. Effects of medial and lateral caudate putamen lesions on place and cue guided behaviors in the water maze: relation to thigmotaxis. *Behav. Brain Res.* **100**, 5 14 (1999).
59. Rauch, T.M., Welch, D.I. & Gallego, L. Hyperthermia impairs retrieval of an overtrained spatial task in the Morris water maze. *Behav. Neural Biol.* **52**, 321 330 (1989).
60. Giese, K.P., Fedorov, N.B., Filipkowski, R.K. & Silva, A.J. Autophosphorylation at Thr^{286} of the α calcium calmodulin kinase II in LTP and learning. *Science* **279**, 870 873 (1998).
61. Guzowski, J.F., Setlow, B., Wagner, E.K. & McGaugh, J.L. Experience dependent gene expression in the rat hippocampus after spatial learning: A comparison of the immediate early genes *Arc, c fos,* and *zif268*. *J. Neurosci.* **21**, 5089 5098 (2001).
62. Brown, R.W. *et al.* Adulthood nicotine treatment alleviates behavioural impairments in rats neonatally treated with quinpirole: possible roles of acetylcholine function and neurotrophic factor expression. *Eur. J. Neurosci.* **19**, 1634 1642 (2004).
63. Wolfer, D.P., Stagljar Bozicevic, M., Errington, M.L. & Lipp, H. P. Spatial memory and learning in transgenic mice: Fact or artifact? *News Physiol. Sci.* **13**, 118 123 (1998).
64. Lipp, H.P. & Wolfer, D.P. Genetically modified mice and cognition. *Curr. Opin. Neurobiol.* **8**, 272 280 (1998).

© 2006 Nature Publishing Group http://www.nature.com/natureprotocols

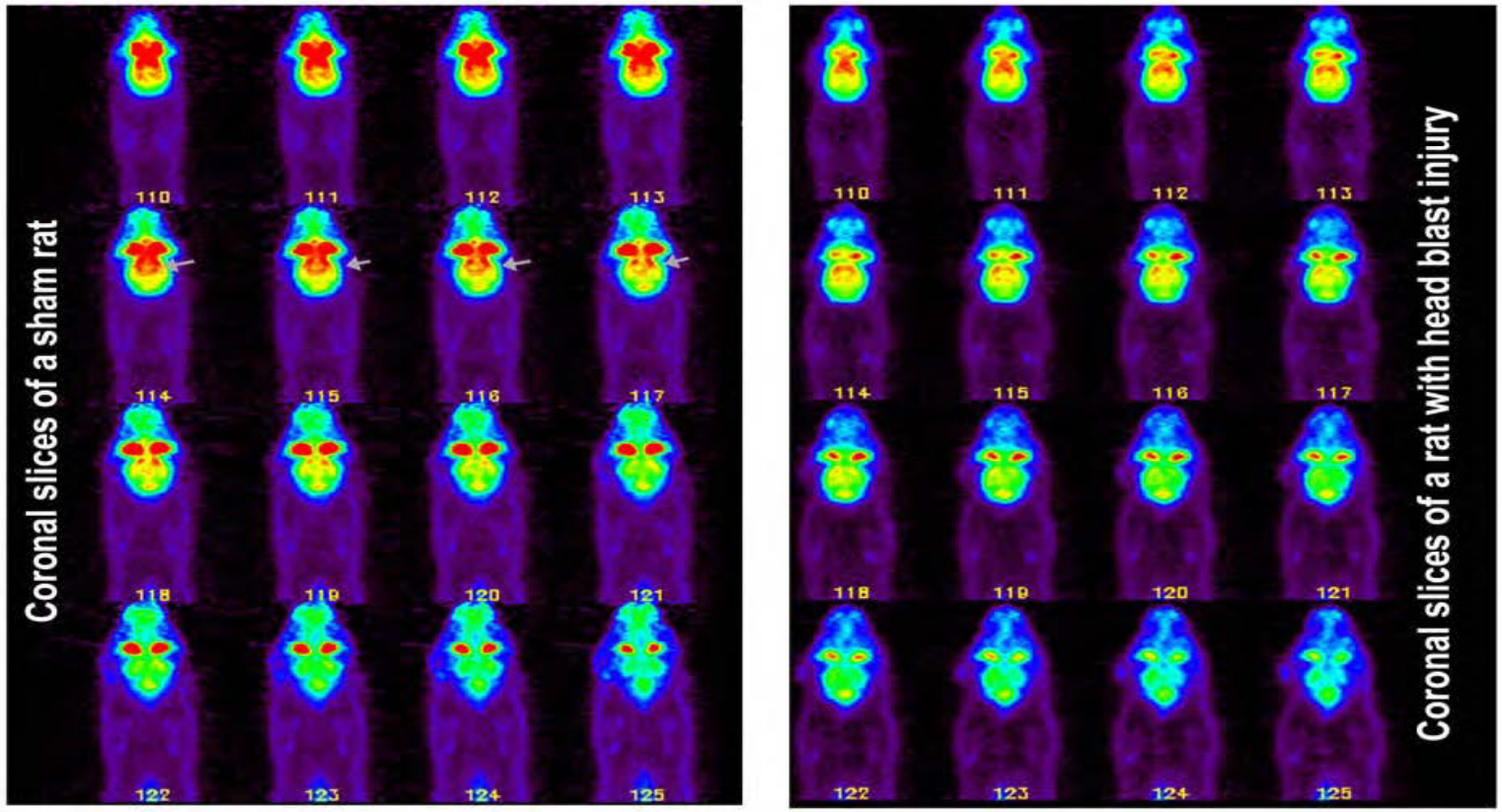

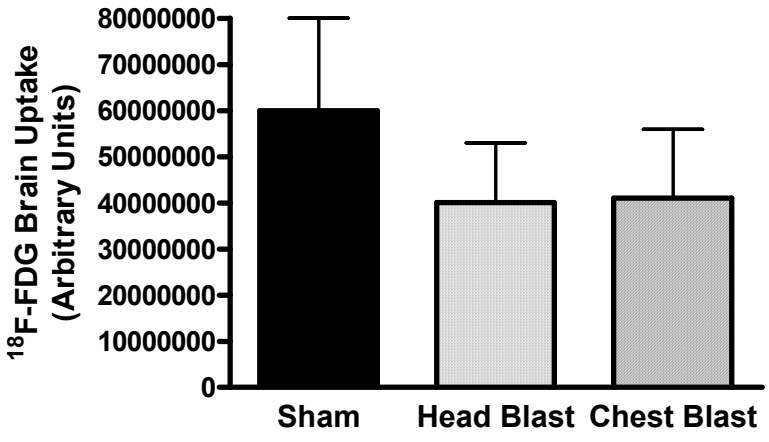

Fig. 11. Blast injury reduces global ^{18}F-FDG uptake in rat brain. Coronal slices of representative rat brains are shown below. The global uptake of the radiotracer was estimated by drawing a region of interest around the entire brain of rats receiving identical radiotracer doses and imaged in an identical manner. The graph represents mean +/- SEM of 3-4 rats/group.

Fig. 14. Activation of RISK signaling cascades following Nociceptin or SNP treatment.

NG108-15 (A) and SH-SY5Y (B) cells were treated in the absence or presence of Noc (1 μM) or SNP (100 μM; positive control) for indicated time points. Cells were serum starved 3 hr prior to 1, 3, 5, 30 and 60 min treatments and concurrently for 3, 6, and 24 hr treatments. These are representative blots of two experiments.

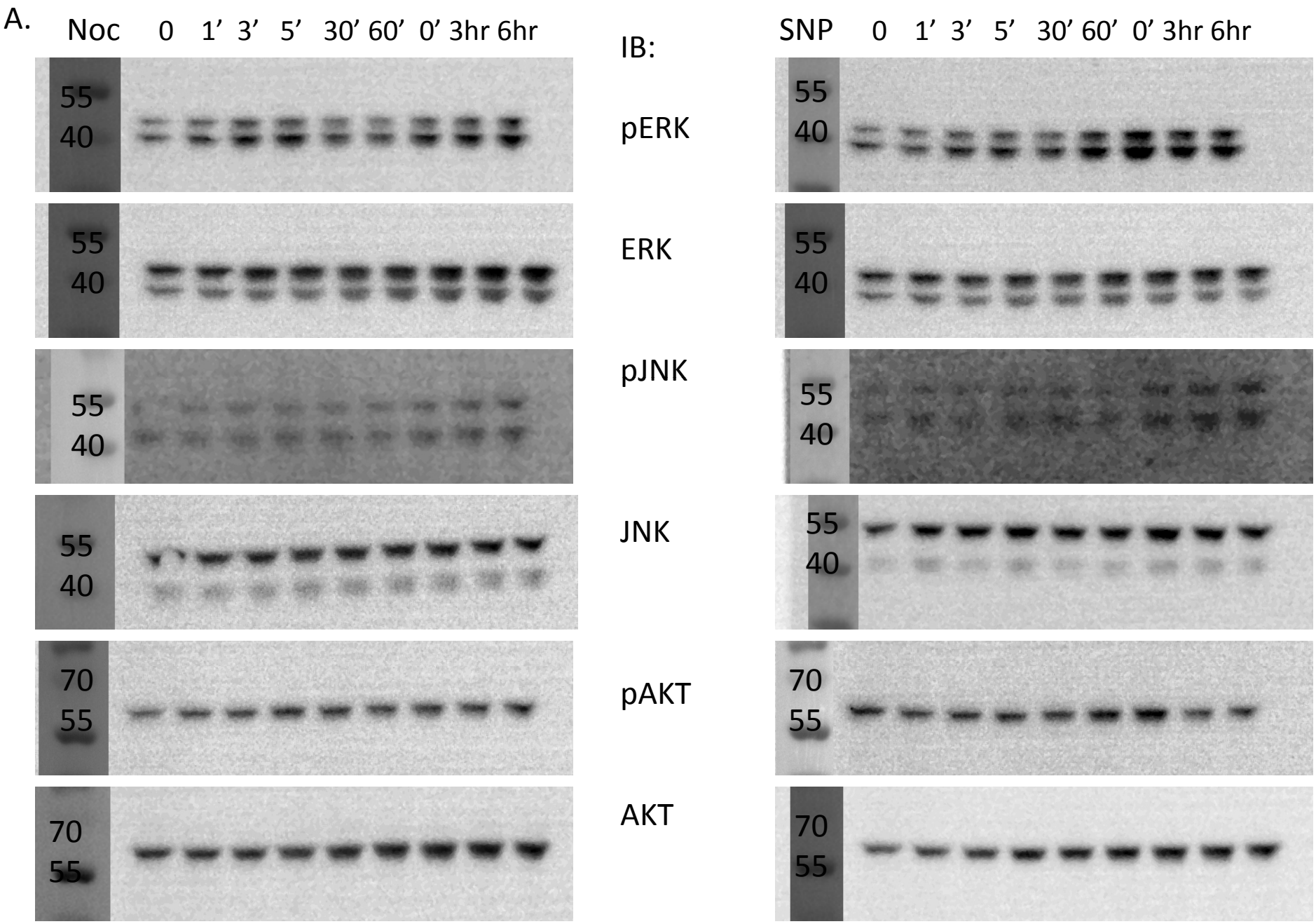
A.
Noc 0 1' 3' 5' 30' 60' 0' 3hr 6hr
SNP 0 1' 3' 5' 30' 60' 0' 3hr 6hr
IB:
pERK
ERK
pJNK
JNK
pAKT
AKT
55
40
70
55

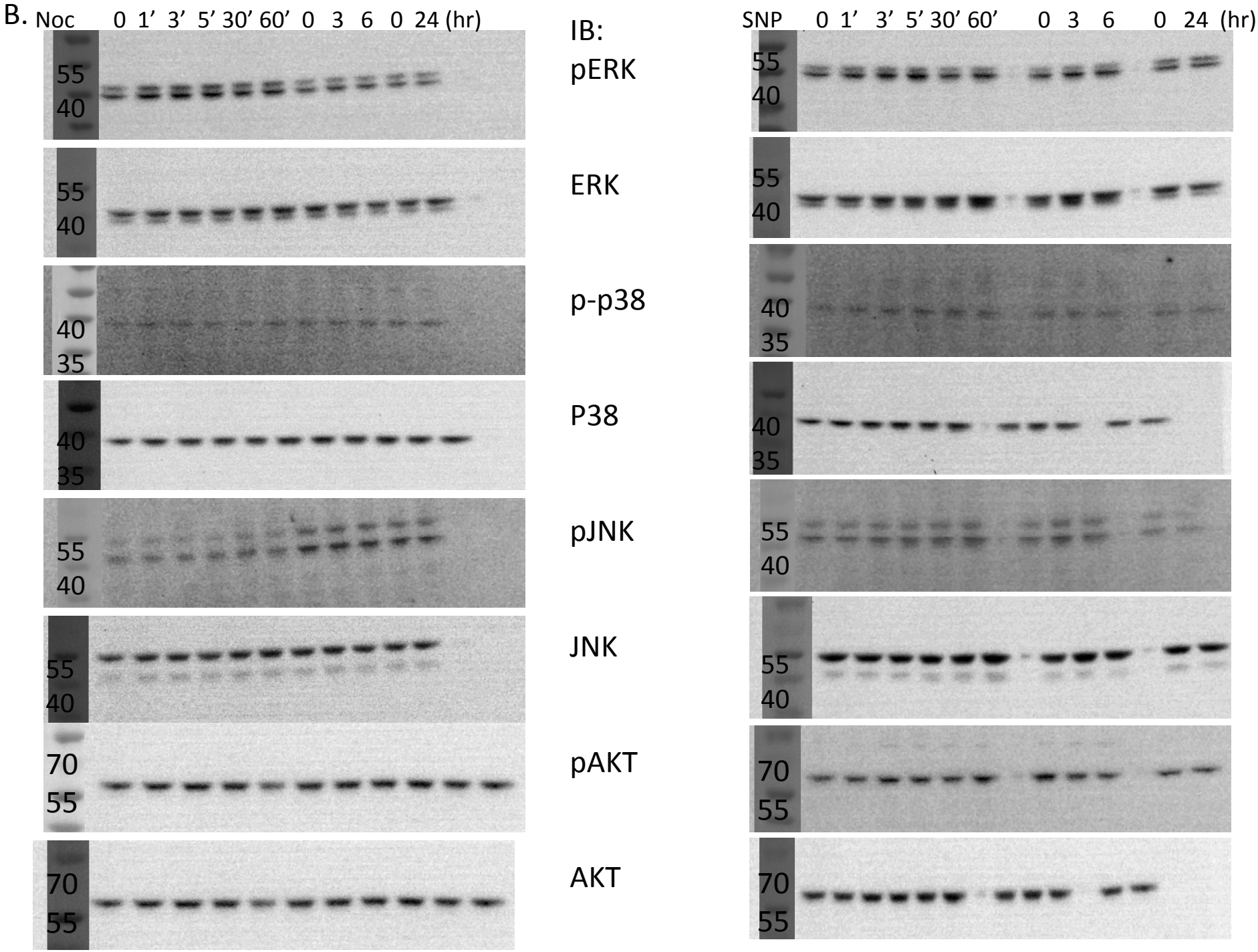
B.
Noc 0 1' 3' 5' 30' 60' 0 3 6 0 24 (hr)
IB:
SNP 0 1' 3' 5' 30' 60' 0 3 6 0 24 (hr)
pERK
ERK
p-p38
P38
pJNK
JNK
pAKT
AKT
55
40
35
70